Environmental Science & Technology

Article

pubs.acs.org/est

High Conservation in Transcriptomic and Proteomic Response of White Sturgeon to Equipotent Concentrations of 2,3,7,8-TCDD, PCB 77, and Benzo[a]pyrene

Jon A. Doering,[*,†,‡] Song Tang,[§] Hui Peng,[‡] Bryanna K. Eisner,[‡] Jianxian Sun,[‡] John P. Giesy,[‡,∥] Steve Wiseman,[‡] and Markus Hecker[*,‡,§]

[†]Toxicology Graduate Program, University of Saskatchewan, 44 Campus Drive, Saskatoon, SK S7N 5B3, Canada

[‡]Toxicology Centre, University of Saskatchewan, 44 Campus Drive, Saskatoon, SK S7N 5B3, Canada

[§]School of Environment and Sustainability, University of Saskatchewan, Saskatoon, SK S7N 5C8, Canada

[∥]Department of Veterinary Biomedical Sciences, University of Saskatchewan, Saskatoon, SK S7N 5B4, Canada

Supporting Information

ABSTRACT: Adverse effects associated with exposure to dioxin-like compounds (DLCs) are mediated primarily through activation of the aryl hydrocarbon receptor (AHR). However, little is known about the cascades of events that link activation of the AHR to apical adverse effects. Therefore, this study used high-throughput, next-generation molecular tools to investigate similarities and differences in whole transcriptome and whole proteome responses to equipotent concentrations of three agonists of the AHR, 2,3,7,8-TCDD, PCB 77, and benzo[a]pyrene, in livers of a nonmodel fish, the white sturgeon (*Acipenser transmontanus*). A total of 926 and 658 unique transcripts were up- and down-regulated, respectively, by one or more of the three chemicals. Of the transcripts shared by responses to all three chemicals, 85% of up-regulated transcripts and 75% of down-regulated transcripts had the same magnitude of response. A total of 290 and 110 unique proteins were up- and down-regulated, respectively, by one or more of the three chemicals. Of the proteins shared by responses to all three chemicals, 70% of up-regulated proteins and 48% of down-regulated proteins had the same magnitude of response. Among treatments there was 68% similarity between the global transcriptome and global proteome. Pathway analysis revealed that perturbed physiological processes were indistinguishable between equipotent concentrations of the three chemicals. The results of this study contribute toward more completely describing adverse outcome pathways associated with activation of the AHR.

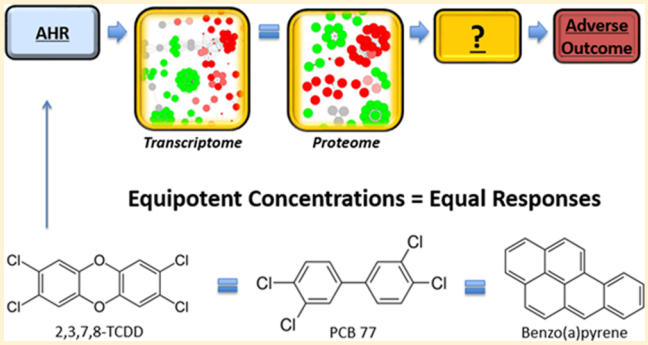

INTRODUCTION

Dioxin-like compounds (DLCs), which include polychlorinated dibenzo-*p*-dioxins (PCDDs), polychlorinated dibenzofurans (PCDFs), and coplanar polychlorinated biphenyls (PCBs), are ubiquitous, persistent, and bioaccumulative pollutants of environmental concern globally. Exposure to DLCs can lead to a variety of adverse effects in vertebrates, with fishes being among the most sensitive. Fishes are particularly sensitive to DLCs during early life stages.[1−9] Adverse effects associated with exposure of early life stages of fishes include craniofacial and cardiovascular malformation, pericardial and yolk sac edema, and posthatch mortality.[10,11] Adverse effects associated with exposure of less sensitive juvenile or adult life stages of fishes primarily include wasting syndrome, fin necrosis, and hepatotoxicity[12−14] but can also include reduced hemopoiesis, hyperplasia of gill filaments, histological lesions, immune suppression, impaired reproductive and endocrine processes, carcinogenesis, and mortality.[11,15−17]

DLCs share similarities in structure and a total of seven PCDDs, ten PCDFs, and 12 PCBs are considered dioxin-like because they bind with relatively great affinity to the aryl hydrocarbon receptor (AHR).[18,19] The AHR is a ligand-activated transcription factor in the basic/helix−loop−helix/Per-ARNT-Sim (bHLH-PAS) family of proteins.[11] Most, if not all, critical adverse effects associated with exposure to DLCs are mediated through activation of the AHR and dysregulation of AHR-responsive genes.[11] Exposure to other anthropogenic contaminants that bind to the AHR, including some polycyclic aromatic hydrocarbons (PAHs), can also result in dioxin-like adverse effects in fishes.[20−23] Since all DLCs exert toxicity via a single, specific mechanism, toxicity of a mixture of DLCs follows an

Received: February 2, 2016
Revised: April 8, 2016
Accepted: April 12, 2016
Published: April 12, 2016

DOI: 10.1021/acs.est.6b00490
Environ. Sci. Technol. 2016, 50, 4826−4835

approximately additive toxicity model.[19] Manifested adverse effects, such as pericardial and yolk sac edema, as well as mortality were indistinguishable between embryos of rainbow trout (*Oncorhynchus mykiss*) exposed to mixtures of DLCs or single DLCs at concentrations that result in equal activation of the AHR.[24,25] Because equipotent concentrations of DLCs result in indistinguishable apical effects in fishes, it would be hypothesized that equal activation of the AHR by any DLC or mixture of DLCs results in indistinguishable response across levels of biological organization (i.e., transcript, protein, tissue).

Despite decades of research into the molecular initiating event (i.e., binding of DLCs to the AHR) and apical adverse effects of DLCs, little is known about the cascade of key events that link activation of the AHR with apical adverse effects, particularly in nonmammalian and nonmodel species. Therefore, in order to investigate these key events and improve linkages between molecular data sets and apical adverse effects of regulatory relevance, this study used high-throughput, next-generation molecular tools as an initial 'proof of concept' for characterizing the similarities (or lack thereof) in acute responses between the transcriptome and proteome to equipotent concentrations of three different agonists of the AHR in livers of juvenile white sturgeon (*Acipenser transmontanus*). White sturgeon are a nonmodel, ecologically relevant, endangered species of fish. White sturgeon have been the focus of a series of recent investigations into responses to DLCs as part of ongoing assessments of risk to white sturgeon in particular and sturgeons in general.[26−30] Specifically, juvenile white sturgeon were exposed to equipotent concentrations of the PCDD, 2,3,7,8-tetrachloro-dibenzo-*p*-dioxin (TCDD), the PCB, 3,3′,4,4′-tetrachlorobiphenyl (PCB 77), and the PAH, benzo[a]pyrene (BaP). TCDD is the prototypical agonist of the AHR, while PCB 77 is as much as 5000-fold less potent than TCDD.[19] BaP is among the strongest agonists of the AHR among the PAHs[31] but can also elicit several non-AHR-mediated adverse effects, including carcinogenic, mutagenic, and immunotoxic effects.[32] Unlike DLCs, BaP can be rapidly metabolized and bioactivated.[32] Therefore, the specific objectives of this study were to 1) determine global responses of the whole transcriptome and proteome; 2) compare responses of the transcriptome to responses of the proteome; and 3) compare perturbation of physiological processes and predict similarities and differences in key events that could result in apical adverse effects on whole organisms.

MATERIALS AND METHODS

Animals. Juvenile white sturgeon of approximately three years of age and ranging in body mass (bm) from 460 to 1512 g were reared from eggs acquired from the Kootenay Trout Hatchery (Fort Steele, BC). The studies reported here were approved by the Animal Research Ethics Board at the University of Saskatchewan (Protocol #20110082). Use of endangered white sturgeon was permitted by Environment Canada (Permit #SARA305).

Intraperitoneal Exposure. The protocol used for exposing white sturgeon has been described previously.[26] In brief, 16 white sturgeon ($n = 4$ per treatment) were randomly assigned to one of four 400 L tanks that were maintained at approximately 12 °C under flow-through conditions. Each individual received one intraperitoneal injection containing either 5 μg of TCDD/kg-bm (purity >98%; Wellington Laboratories, Guelph, ON), 5 mg of PCB 77/kg-bm (purity 100%; Chromographic Specialties, Brockville, ON), or 30 mg of BaP/kg-bm (purity ≥96%; Sigma-Aldrich, Oakville, ON) in corn oil. Control individuals received corn oil alone. Doses were chosen to represent equally potent concentrations of each chemical based on maximal activation of the AHR as determined during previous *in vitro* and *in vivo* investigations of sensitivity of white sturgeon to agonists of the AHR[26,27,29,30] and represent the lowest observed effect concentration (LOEC) in rainbow trout 4 weeks after treatment.[33] Three days following injection, livers from all individuals were excised and frozen in liquid nitrogen.

Transcriptomics. A detailed description of transcriptomic sample preparation, sequencing, and data analysis is available in the Supporting Information. In brief, total RNA was extracted from each individual. Only samples with an RNA Integrity Number (RIN) ≥ 8 were used in subsequent analysis (Control $n = 3$; TCDD, PCB 77, and BaP $n = 4$). Equal amounts of RNA from each individual were pooled to create one RNA-Seq library per treatment. Each library was loaded onto a separate Mi-Seq v3 150 cycle cartridge (*Illumina*, San Diego, CA) and run as 75 base-pair (bp) paired-end reads on a Mi-Seq sequencer (*Illumina*) at the Toxicology Centre (University of Saskatchewan, Saskatoon, SK). Raw sequences have been made available in the National Center for Biotechnology Information (NCBI) Gene Expression Omnibus (GEO) (Accession #GSE79624).

No public databases for either the genome or transcriptome of white sturgeon were available. Therefore, a comprehensive reference transcriptome was constructed by use of *de novo* assembly from reads for liver of white sturgeon described here and in earlier studies described elsewhere.[28] The reference transcriptome has been made available in the NCBI GEO (Accession #GSE79624). Reads comprising each treatment were aligned to the reference transcriptome. Since statistical analysis cannot be conducted on the pooled libraries, significance of differentially expressed transcripts was scored by a change in abundance greater than or equal to a threshold of ±2-fold relative to abundance in controls. Further, results of transcriptome analysis for a subset of six genes (Table S1) was validated by use of quantitative real-time polymerase chain reaction (qRT-PCR). This analysis showed a significant and positive linear relationship between results of transcriptome analysis and results of qRT-PCR across all chemicals and genes ($R^2 = 0.92$, $p < 0.0001$, Figure S1, Table S2). Variance among the three control individuals was also demonstrated to be minimal with an average standard deviation (SD) of ±41% of abundance of the mean ($n = 3$) across the subset of six genes (Table S3).

Proteomics. A detailed description of proteomic sample preparation, sequencing, and data analysis is available in the Supporting Information. In brief, livers from individuals of each treatment group were pooled at equal mass to create one sample per treatment (Control $n = 3$; TCDD, PCB 77, and BaP $n = 4$). Pooled livers were homogenized and digested. Each prepared sample was loaded in duplicate onto a 75 mm inner diameter fused silica microcapillary column (Polymicron Technologies, Phoenix, AZ) packed with 10 cm of Luna 3-mC18 100 Å reversed phase particles (Phenomenex, Torrance, CA) and placed in-line with a nanoLC-electrospray ion source (Proxeon, Mississauga, ON) interfaced to an LTQ Orbitrap Velos hybrid mass spectrometer (Thermo Fisher Scientific, Waltham, MA) at the University of Toronto (Toronto, ON). Raw MS/MS sequences have been deposited to the ProteomeXchange Consortium via the Proteomics Identifications (PRIDE) partner repository (Accession #PXD003840).[34] No public databases for proteome sequences of white sturgeon were available. Therefore, a comprehensive, genome-free, artifact-free reference proteome

DOI: 10.1021/acs.est.6b00490
Environ. Sci. Technol. 2016, 50, 4826−4835

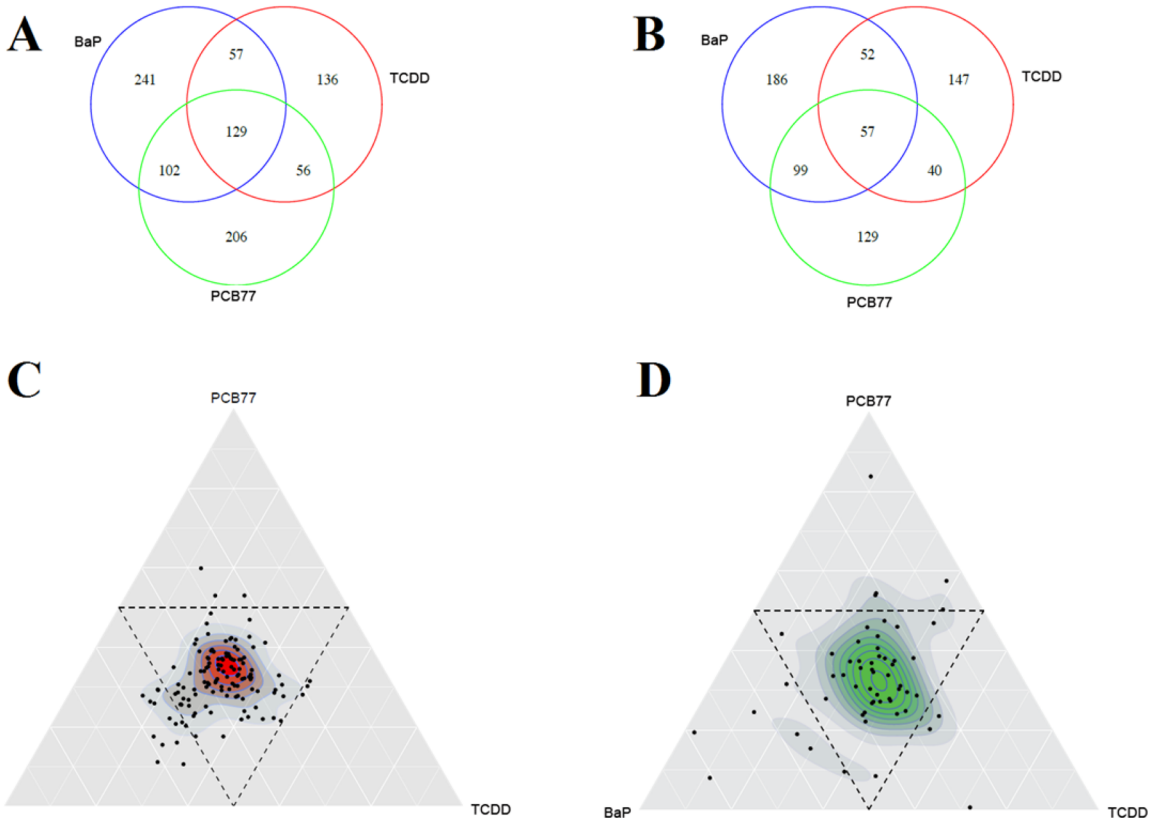

Figure 1. Venn diagrams representing number of transcripts with increased abundance (A) and number of transcripts with decreased abundance (B) based on transcriptome responses in livers of white sturgeon exposed to TCDD (red), PCB 77 (green), and BaP (blue). Density ternary plots representing transcripts with increased abundance (C) and transcripts with decreased abundance (D) shared by TCDD, PCB 77, and BaP. Each dot (black) represents a transcript with 129 transcripts represented in (C) and 57 transcripts represented in (D). The position of a transcript is specified as the center of mass (barycenter) of masses placed at the vertices of an equilateral triangle, and the proportions of the three treatments sum to 100%. Each point represents a different composition of the three treatments, with the maximum proportion (100%) of each treatment in each corner of the triangle and the minimum proportion (0%) at the opposite line. Color gradient represents kernel density estimation for up-regulated (red) and down-regulated (green) transcripts. Dashed lines border the barycenter which contains transcripts with equal fold-change following exposure to TCDD, PCB 77, or BaP. Transcripts outside of the dashed lines had greater fold-change following exposure to the chemical in the corresponding corner relative to the other chemicals.

was constructed based on the liver transcriptome of white sturgeon through the online pipeline at http://kirschner.med.harvard.edu/tools/mz_ref_db.html.[35] The reference proteome has been made available in the PRIDE partner repository (Accession #PXD003840). Sequences comprising each treatment were aligned to the reference proteome. Since statistical analysis cannot be conducted on the pooled samples, significance of differentially expressed proteins was scored by a change in abundance greater than or equal to a threshold of ±2-fold relative to controls.

Data Analysis. Associations between multivariate descriptors of expression of transcriptome (69 312 contigs) and proteome (520 proteins) were inferred by use of coinertia analysis (CIA).[36] A Monte Carlo test with 5000 permutations was used for validating results of CIA. Software packages used in data analysis are described in the Supporting Information.

Pathway Analysis. Pathway analyses (functional grouped Gene Ontology (GO) terms analysis) were visualized by use of ClueGO v.2.1.6[37] run through Cytoscape v.3.2.1[38] by use of ontologies based on zebrafish in the Kyoto Encyclopedia of Genes and Genomes (KEGG) and the GO Consortium Biological Processes.

RESULTS AND DISCUSSION

Equipotent Concentrations of TCDD, PCB 77, and BaP. The AHR is conserved among vertebrate taxa and is best known for its ability to regulate expression of cytochrome P450 1A (CYP1A) as part of an adaptive response to exposure to certain xenobiotics.[39] Equipotent concentrations of TCDD, PCB 77, and BaP increased abundance of transcripts of CYP1A relative to controls ($p \leq 0.05$), but there were no statistical differences among these treatments ($p > 0.05$) (Figure S2). This indicated approximately equal activation of the AHR and suggests that approximately equipotent concentrations were administered, although a full dose−response would be required to confirm this hypothesis. Further, prior studies on white sturgeon have shown maximal abundance of transcripts of CYP1A to range from approximately 10- to 20-fold greater than controls following exposure to DLCs, with abundance of transcripts of CYP1A in the study presented here being 25-, 15-, and 24-fold greater than controls for TCDD, PCB 77, and BaP, respectively (Figure S2).[26,30] This indicates that approximately maximal response of activation of the AHR was achieved by exposure to each of the three chemicals.

Comparison among Responses to TCDD, PCB 77, and BaP. Abundances of 674, 818, and 923 transcripts were altered by ≥2-fold relative to controls in livers of white sturgeon exposed

DOI: 10.1021/acs.est.6b00490
Environ. Sci. Technol. 2016, 50, 4826−4835

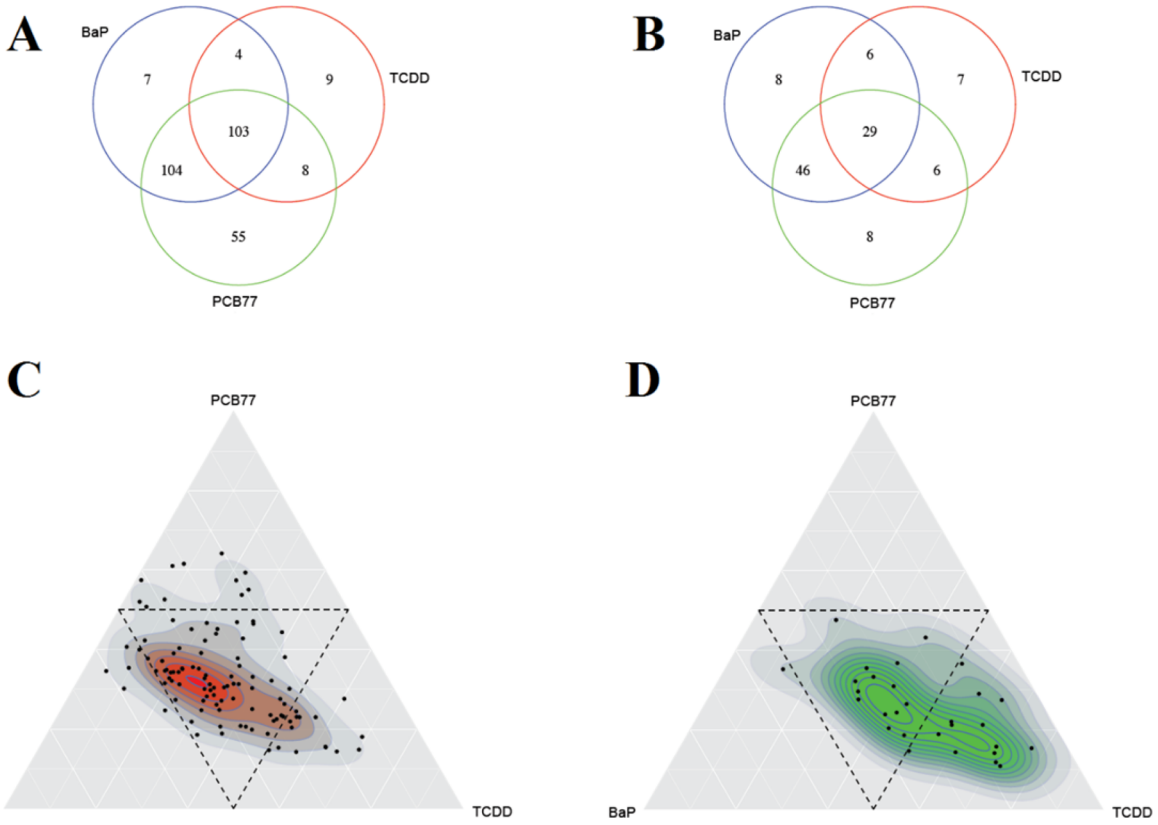

Figure 2. Venn diagrams representing number of proteins with increased abundance (A) and number of proteins with decreased abundance (B) based on proteome responses in livers of white sturgeon exposed to TCDD (red), PCB 77 (green), and BaP (blue). Density ternary plots representing proteins with increased abundance (C) and proteins with decreased abundance (D) shared by TCDD, PCB 77, and BaP. Each dot (black) represents a protein with 103 proteins represented in (C) and 29 proteins represented in (D). The position of a protein is specified as the center of mass (barycenter) of masses placed at the vertices of an equilateral triangle, and the proportions of the three treatments sum to 100%. Each point represents a different composition of the three treatments, with the maximum proportion (100%) of each treatment in each corner of the triangle and the minimum proportion (0%) at the opposite line. Color gradient represents kernel density estimation for up-regulated (red) and down-regulated (green) proteins. Dashed lines border the barycenter which contains proteins with equal fold-change following exposure to TCDD, PCB 77, or BaP. Proteins outside of the dashed lines had greater fold-change following exposure to the chemical in the corresponding corner relative to the other chemicals.

to TCDD, PCB 77, and BaP, respectively (Table S4). Of the altered transcripts, 378, 493, and 529 were increased while 296, 325, and 394 were decreased by TCDD, PCB 77, and BaP, respectively (Table S4). Few studies to date have investigated responses to activation of the AHR across the whole transcriptome, particularly in nonmodel and nonmammalian species; and no studies have investigated whole proteome responses. One commonality among the few studies conducted to date is the great number of genes and physiological processes that were altered, either directly or indirectly, as a result of activation of the AHR. Abundances of 2000 altered transcripts were detected by use of microarray in embryos of zebrafish exposed to TCDD,[40] and 1058 altered transcripts were detected by use of serial analysis of gene expression (SAGE) sequencing in livers of adult zebrafish exposed to TCDD.[41] In studies with embryos of killifish (*Fundulus heteroclitus*), 1167 altered transcripts were detected by use of microarray after exposure to 3,3′,4,4′,5-pentachlorobiphenyl (PCB 126),[42] and 1392 altered transcripts were detected by use of Mi-Seq sequencing in livers of juvenile roach (*Rutilus rutilus*) exposed to TCDD.[43] Less is known regarding responses of the transcriptome or proteome of fishes following exposure to PAHs. However, abundances of 241 altered transcripts were detected by use of microarray in one study on embryos of zebrafish exposed to BaP.[44]

Because the equipotent concentrations that were used caused an approximately equal activation of the AHR, it was hypothesized that global responses of the transcriptome would be similar among chemicals. These responses would then be predicted to result in similar responses at the level of the proteome and then eventually result in similar apical adverse effects and severity of adverse effects at the level of the whole organism. At the level of the transcriptome, expression of a total of 926 unique transcripts was up-regulated by ≥2-fold relative to controls by TCDD, PCB 77, or BaP; but only 14% (129) of these transcripts were common to responses to all three chemicals, and 37% (344) of these transcripts were common to responses to two or more chemicals (Figure 1A). A total of 658 unique transcripts were down-regulated by ≥2-fold relative to controls by TCDD, PCB 77, or BaP, with 9% (57) of these transcripts being common to responses to all three chemicals and 38% (248) of these transcripts being common to responses to two or more chemicals (Figure 1B). Variability at the level of the transcriptome might be expected, and it was hypothesized that numerous changes in abundances of transcripts were likely due to effects not mediated by the AHR and could represent compensatory responses; however, some evidence supports agonist-dependent responses despite the same mode of action.[43,45,46] Transcripts for which expression was altered by all three chemicals might represent core genes of the AHR-gene battery, and, therefore, these

DOI: 10.1021/acs.est.6b00490
Environ. Sci. Technol. 2016, 50, 4826−4835

transcripts were plotted in a density ternary plot incorporating fold-change in order to determine whether shared transcripts had similar magnitudes of response to equipotent concentrations as would be expected for core genes in the AHR-gene battery (Figure 1C; 1D). Of the 129 and 57 shared up- and down-regulated transcripts, 85% (110) and 75% (43), respectively, clustered in the middle of the ternary plot indicating that equipotent concentrations of each chemical caused comparable fold-changes in expression at the level of the transcriptome. Equal magnitudes of responses at equipotent concentrations of each chemical were confirmed by qRT-PCR for six selected genes. No statistically significant differences ($p > 0.05$) were detected between response to TCDD, PCB 77, and BaP for CYP1A (Figure S2), aryl hydrocarbon receptor repressor (AHRR) (Figure S3), fructose-1,6-bisphosphatase 1a (FBP1A) (Figure S4), superoxide dismutase (SOD) (Figure S5), sex determining region Y-box 9 (SOX9) (Figure S6), or cholesterol 7-alpha-monooxygenase 1a (CYP7A1A) (Figure S7). Similar magnitudes of responses for the majority of shared transcripts due to exposure to equipotent concentrations of the three chemicals support the hypothesis that these transcripts might represent core genes of the AHR-gene battery.

Compared to changes across the transcriptome, fewer proteins were altered in livers of white sturgeon across the proteome. A total of 282, 359, and 307 proteins were altered by ≥2-fold relative to controls by TCDD, PCB 77, and BaP, respectively (Table S4). A greater number of proteins were up-regulated by TCDD, PCB 77, and BaP (180, 270, and 218, respectively) than were down-regulated (102, 89, and 89, respectively) (Table S4). A total of 290 unique proteins were up-regulated by ≥2-fold relative to controls by TCDD, PCB 77, or BaP, with 36% (103) and 76% (219) of these proteins being common to all three or to two or more chemicals, respectively (Figure 2A). A total of 110 unique proteins were down-regulated by ≥2-fold relative to controls by TCDD, PCB 77, or BaP, with 26% (29) and 76% (87) of these proteins being common to all three or to two or more chemicals, respectively (Figure 2B). Of the 103 shared proteins that were up-regulated by each of the three chemicals, 70% (72) were clustered in the middle of the ternary plot (Figure 2C); and of the 29 proteins that were down-regulated by each of the three chemicals, 48% (14) were clustered in the middle of the ternary plot (Figure 2D) indicating comparable fold-changes in abundances of proteins in response to equipotent concentrations of the three chemicals. As with the transcriptome, the similar magnitude of response for the majority of shared proteins by equipotent concentrations of the three chemicals supports the hypothesis that these proteins might represent core genes of the AHR-gene battery.

Comparison between the Global Transcriptome and Global Proteome. Although transcripts are a prerequisite for translation of genes to proteins, there is uncertainty regarding whether altered abundance of transcripts has functional consequence at the level of the cell, tissue, or whole organism. Therefore, changes in abundances of transcripts were compared to changes in abundances of proteins. Across treatments there was 68% similarity between the global transcriptome and global proteome (Figure 3). This is in contrast to some studies comparing global transcriptomes with global proteomes that have reported weak correlations as a result of post-translational effects.[47] Investigations at the protein level are considered more representative of dysregulation of physiology of organisms relative to investigations at the transcript level.[48] Due to covariation between the transcriptome and proteome, this

Figure 3. Association between transcriptomes and proteomes by use of coinertia analysis (CIA) of transcriptome (red circle) and proteome (green triangle) responses in livers of white sturgeon following exposure to TCDD, PCB 77, or BaP. CIA is a multivariate method that identifies trends or corelationships in multiple data sets. Global similarity (coinertia) between transcriptomic and proteomic data sets is 68% ($p = 0.1639$).

indicates that responses to activation of the AHR at the level of the transcriptome are largely representative of responses of the proteome. It is hypothesized that this agreement between changes that translate across levels of molecular organization (i.e., transcriptome to proteome) could be indicative of further downstream physiological alterations representing apical adverse effects at the level of the whole organism.

Perturbations Among Physiological Pathways. The AHR-gene battery up-regulates genes in response pathways involved in response to xenobiotics, including CYP1A, aldehyde dehydrogenases (ADH), glutathione *S*-transferases (GST), NAD(P)H quinone oxidoreductases (NQO), and UDP-glucuronosyltransferases (UGT), as well as the AHRR.[49−51] Responses of both the transcriptome and proteome in livers of white sturgeon exposed to TCDD, PCB 77, or BaP included greater abundances of transcripts and proteins in these response pathways relative to controls, including genes such as CYP1, CYP2, CYP3, UGT, GST, sulfotransferases (SULT), and AHRR (Figures 4; S2; S3; Data set S1; Data set S2). Due to the great increase in expression of Phase I enzymes in response to exposure to DLCs, oxidative stress as a result of chronic, increased expression of CYPs has been proposed as a mode of action for toxicity of DLCs.[52] However, antisense repression of CYP1s fails to prevent developmental toxicity of TCDD, which indicates that toxicity of AHR-agonists is predominantly due to CYP-independent mechanisms,[53] and therefore necessitates further investigation into the modes of action for toxicity by DLCs.

Despite an important role in responses to exposure to xenobiotics, it has been proposed that ancestral functions of the

DOI: 10.1021/acs.est.6b00490
Environ. Sci. Technol. 2016, 50, 4826−4835

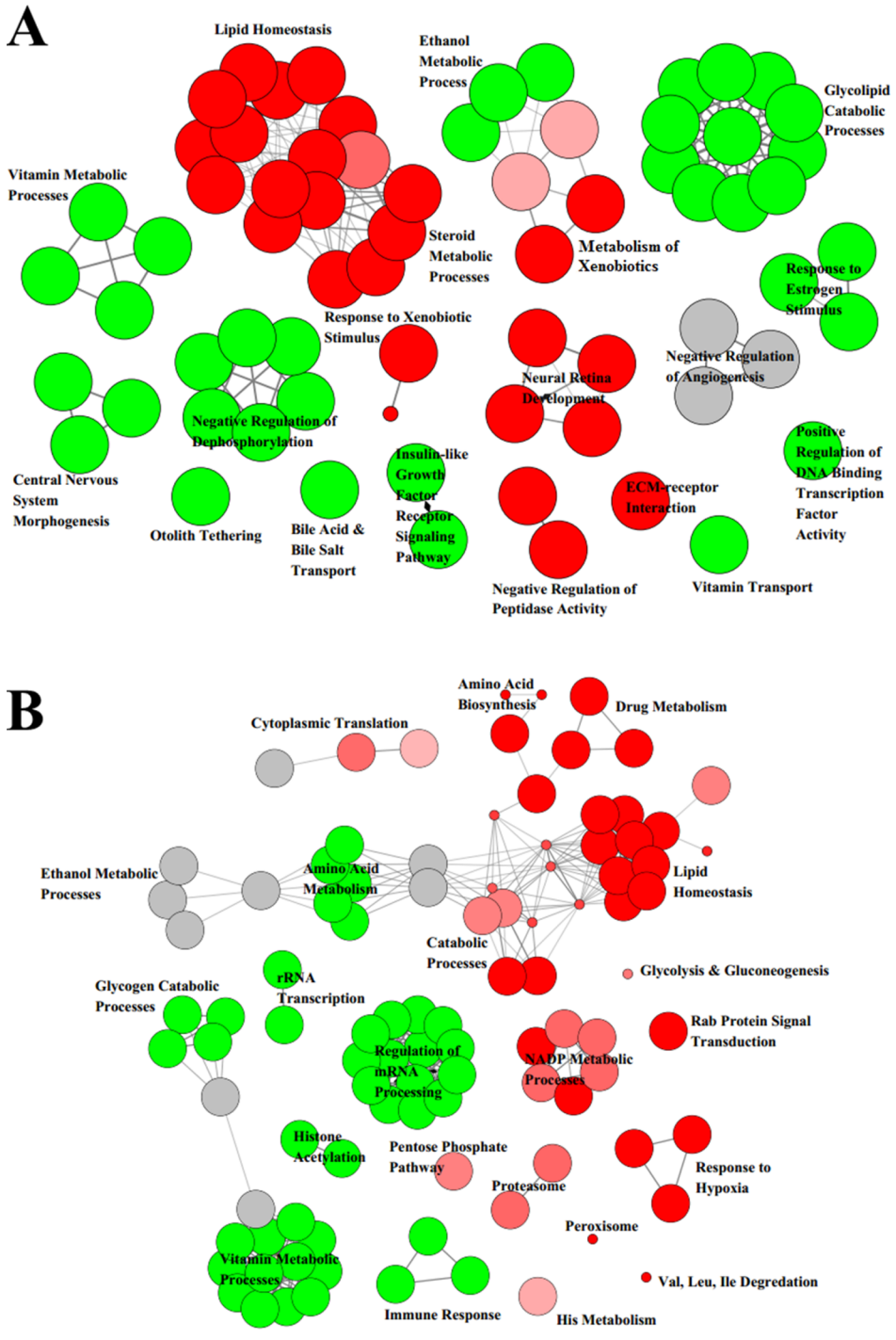

Figure 4. Cytoscape visualization of ClueGO clustering results of shared physiological processes altered by TCDD, PCB 77, and BaP at the level of the transcriptome (A) and proteome (B) in livers of white sturgeon. Clusters with a greater proportion of up-regulated processes are shown in red, while clusters with a greater proportion of down-regulated processes are shown in green. Degree of red or green shows relative abundance of up-regulated vs down-regulated processes in each cluster. Gray clusters consist of 50% up-regulated processes and 50% down-regulated processes. Size of cluster represents the relative number of processes in the cluster. Interconnection between pathways is represented by gray interconnecting lines indicating that these categories share transcript(s) or protein(s). The statistical test was set to a right-sided hypergeometrical test with a Bonferroni (step down) *p*-value correction and a *kappa* score of 0.4. Response pathways for shared genes are representative of complete response pathways for individual chemicals, namely TCDD (Figure S8), PCB 77 (Figure S9), and BaP (Figure S10).

AHR were regulation of developmental and regenerative processes of liver, immune system, gonad, heart, and sensory systems.[39] Therefore, potent activation of the AHR by agonists could result in dysregulation of a range of critical developmental and homeostatic processes in embryos, juveniles, and adults. One example is the wingless-type MMTV integrated site family (WNT) signaling pathway, which has been proposed as a critical target of the AHR.[54,55] WNTs are a large family of proteins that are highly conserved across taxa and play important roles in development and maintaining normal homeostasis by regulating cell proliferation through control of cell cycle regulators.[55] Dysregulation of WNT signaling, and the interrelated Hedgehog

DOI: 10.1021/acs.est.6b00490
Environ. Sci. Technol. 2016, 50, 4826−4835

(HH) signaling pathway, lead to a variety of adverse effects, including carcinogenesis and developmental deformities, making negative or positive feedback control of WNT signaling critical for proper functioning of an organism.[54,55] Expression of several transcripts in the WNT signaling pathway, including WNT5B and Indian hedgehog (IHH) A, was up-regulated at the level of the transcriptome by TCDD, PCB 77, and BaP (Data set S1). Pathway analysis indicated that dysregulation of the WNT signaling pathway might have affected several developmental processes, including those involved with the sensory and lateral line systems, neuromast development, tissue and fin regeneration and wound healing, development of the endocrine pancreas, and endocrine and cardiovascular systems, angiogenesis and development of blood vessels, somite development, and axis elongation, among others (Figures 4; S8; S9; S10; Data set S2). Several other signaling pathways have also been suggested to be regulated by the AHR or altered through cross-talk, including the pregnane X receptor (PXR), endocrine, hypoxia, and peroxisome proliferation-activated receptor (PPAR) signaling pathways.[10,56,57] Responses of the transcriptome in liver of white sturgeon exposed to TCDD, PCB 77, and BaP included up-regulation of key nuclear receptors representative of several of these signaling pathways, including, AHR1 and AHR2, PPAR, androgen receptor (AR), and hypoxia inducible factor-1α (HIF-1α) (Data set S1). However, nuclear receptors were not detected in the proteome, mainly due to their low abundance which could not be detected by the present proteomic analytical method. Taken together, this indicates possible dysregulation of several critical developmental and homeostatic processes that could lead to a range of adverse effects, including deformities, endocrine disruption, carcinogenesis, and impaired growth and reproduction.

Widespread changes in expressions of genes have been suggested to be a likely reason for pleiotropic apical adverse effects associated with activation of the AHR.[40,41,45] However, it is also thought that most AHR-responsive genes play no direct role in mediating apical adverse effects and that only a core of species- and chemical-independent genes, which share common functions, is responsible for observed toxicities.[47] In the study presented here, 129 up-regulated and 57 down-regulated genes were observed at the level of the transcriptome (Figure 1) and 103 up-regulated and 29 down-regulated proteins were observed at the level of the proteome (Figure 2) that were common to all three chemicals. These transcripts and proteins were used to identify physiological processes regulated directly by activation of the AHR (Figure 4). Pathway analysis of these altered transcripts and proteins indicated that similar physiological processes were perturbed at both the level of the transcriptome (Figure 4A) and proteome (Figure 4B), including processes that were identified in other studies by use of transcriptome analysis.[40,41,43] These processes included responses to xenobiotics, lipid and carbohydrate homeostasis, developmental and regenerative processes, and processes involved with transcription and translation of genes. Further, the major physiological processes that were perturbed by all three chemicals at the level of both the transcriptome and proteome were similar to the processes that were perturbed when all transcripts or proteins altered by TCDD, PCB 77, or BaP at the level of the transcriptome or proteome were analyzed individually (Figures 4; S8; S9; S10). These results support the hypothesis that the AHR mediates widespread perturbation through direct or indirect control over a large number of genes.

The zebrafish has been used as a model fish to successfully elucidate specific mechanisms for several of the classical adverse effects associated with exposure of early life stages of fishes to DLCs. Specifically, craniofacial malformations of zebrafish have been shown to be caused through dysregulation of genes involved in development of skeletal elements, namely down-regulation of sonic hedgehog (SS) A and B and SOX9B and up-regulation of forkhead box (FOX) Q1A.[57−59] Also, cardiovascular malformations in zebrafish have been shown to be caused through dysregulation of genes involved in development of the heart and vasculature, namely up-regulation of cytochrome *c* oxidase (COX) 2 and bone morphogenetic protein (BMP) 4 and down-regulation of the cell cycle gene cluster.[60−62] Less is known regarding specific mechanisms of adverse effects of DLCs on juvenile or adult fishes. However, hepatic steatosis is believed to result from AHR mediated up-regulation of fatty acid translocase (FAT) and PPARα.[63] SS was not identified in the transcriptome or proteome of white sturgeon, while COX and BMP had several isoforms that were unaltered by any of the three chemicals (Data set S1). However, in agreement with results of previous studies of zebrafish, SOX9 was down-regulated and FOX was up-regulated at the level of the transcriptome by all three chemicals in livers of white sturgeon (Data set S1). Although PPARα was not altered, PPARδ was up-regulated at the level of the transcriptome by all three chemicals which is in agreement with previously demonstrated modes of toxic action for hepatic steatosis (Data set S1).[63] FAT was not identified in the transcriptome or proteome of white sturgeon; however, physiological processes involved in lipid homeostasis that are likely to be under control of PPAR and interrelated with FAT were altered at both the level of the transcriptome and the proteome (Data set S1). However, there is uncertainty in the accuracy of genome-free transcriptome or proteome sequencing to identify transcripts or proteins to the isoform level. Therefore, IHH, FOX, SOX, COX, BMP, and PPAR transcripts might be identified as the wrong isoform, which could alter interpretation of predicated perturbation to physiological processes or magnitude of response to exposure to chemicals. These uncertainties at the level of the exact transcript or protein highlight the advantage of investigating entire physiological pathways by use of whole transcriptome or proteome analysis as opposed to investigating individual genes. Also, individual genes affected by each DLC were not always identical; however, the same major processes were perturbed by equipotent concentrations of all three chemicals when entire physiological pathways were considered, which provides confidence in the whole pathway analysis approach.

BaP can also exert effects that are independent of the AHR.[32] Therefore, it was hypothesized that some responses to BaP at the level of the transcriptome and proteome would be unique from responses to TCDD and PCB 77. All, or most, of these non-AHR-mediated effects are believed to be caused by metabolites of BaP that are formed by reactions catalyzed by CYP enzymes.[64] Most effects of BaP have been tested only in species such as mice (*Mus musculus*) and rainbow trout, which have greater rates of CYP-mediated biotransformation relative to other species.[31,65] However, the rate of CYP-mediated biotransformation in liver of white sturgeon has been shown to be slower than in other fishes.[65] Previously, PAHs have been classified based on their potency for causing carcinogenesis, which is believed to be mediated largely through non-AHR-mediated pathways;[31] however, carcinogenesis is not an end point of regulatory relevance in context with the risk assessment of fishes. In the current study, physiological processes that were perturbed by

DOI: 10.1021/acs.est.6b00490
Environ. Sci. Technol. 2016, 50, 4826−4835

BaP did not differ from those of individuals exposed to TCDD or PCB 77, which suggests that activation of the AHR is likely to be the predominant driver of acute responses to exposure to BaP in white sturgeon. However, responses of the transcriptome and proteome might become less similar over time as reactive metabolites of BaP are formed and result in a greater non-AHR-mediated response. If BaP does elicit predominantly AHR-mediated effects on some fishes, it would support the development of toxic equivalency factors (TEFs) for certain PAHs, similar to those currently used for DLCs.[19] However, the weighted importance of AHR-mediated effects relative to non-AHR-mediated effects in eliciting acute or chronic apical adverse effects associated with exposure to PAHs remains unclear, especially among fishes.[21]

Toward Predicting Apical Adverse Effects in Fishes. Recently, there has been an increasing desire to make better use of growing quantities of mechanistic toxicology data (including both transcriptomics and proteomics) in support of chemical risk assessment and regulatory decision making.[66] One approach that has been proposed in this context and that is increasingly gaining acceptance across the scientific and regulatory communities is that of the adverse outcome pathway (AOP). An AOP is a conceptual framework that establishes biologically plausible links between molecular-level perturbation of a biological system and an adverse outcome of regulatory relevance, such as survival, growth, or reproduction.[67] However, due to the complexity of AHR-mediated responses and how they are related to or are linked with adverse outcomes, no complete AOPs are currently available for activation of the AHR (https://aopkb.org/aopwiki/index.php/AOP_List). Toward the objective of describing more complete AOPs associated with activation of the AHR, the study presented here demonstrated three main contributions: 1) AOPs by definition are not chemical specific, and any chemical that triggers the molecular initiating event (i.e., activation of the AHR) should elicit the same chain of downstream key events given equal potency at the molecular initiating event and similar adsorption, distribution, metabolism, and elimination (ADME).[66] It could be demonstrated that equal activation of the AHR by three different agonists (Figure S2) resulted in similar global responses and magnitude of responses at both the level of the transcriptome (Figure 1) and the proteome (Figure 2) and would be predicted to result in similar adverse outcomes and severity of adverse outcomes (Figure 4). It was also demonstrated that where differences existed with regard to the exact transcripts or proteins that were altered, the actual physiological processes that were perturbed were indistinguishable (Figures 4; S8; S9; S10). Therefore, future AOPs developed for activation of the AHR will likely be common to all DLCs and other agonists of the AHR at different levels of biological organization, given equal activation of the AHR and comparable ADME. 2) Key events and the linking key event relationships are not unique to a single AOP or to a single chemical or chemical class.[66] Therefore, common key events are reusable and do not need to be generated independently for each new AOP.[66] Results of the study presented here demonstrated perturbed physiological processes and their associated pathways common to all three chemicals which are likely to represent core perturbations for activation of the AHR (Figure 4). Some of these pathways are well understood, including the WNT, PPAR, HH, ER, AR, and hypoxia pathways, supporting the development of putative AOPs associated with perturbation of these critical pathways as a result of activation of the AHR. However, the link between activation of the AHR and perturbation of these pathways remains an ongoing question. 3) AOPs are not static, and there is no benchmark for when an AOP is complete.[66] AOPs and the associated key events and key event relationships are able to grow over time as new information is generated. Therefore, in order for results of the study presented here to inform future investigation into AOPs associated with activation of the AHR, all data has been made available online for investigation into all transcripts and proteins altered by each of the three chemicals but also the associated physiological processes for each transcript or protein and the fold-change relative to abundances in the control (Data set S1; Data set S2). As such, this comprehensive transcriptomic and proteomic data set will be able to support as yet unrevealed or unexpected biological connections between molecular level perturbations in livers of fishes by DLCs and certain PAHs as a result of activation of the AHR.

■ ASSOCIATED CONTENT

Supporting Information

The information is available free of charge via the Internet at http://pubs.acs.org/. The Supporting Information is available free of charge on the ACS Publications website at DOI: 10.1021/acs.est.6b00490.

Materials and methods, Tables S1−S4, and Figures S1−S10 (PDF)

Whole data set for transcriptomics and proteomics (XLSX)

Whole data set for pathway analysis (XLSX)

■ AUTHOR INFORMATION

Corresponding Authors

*Phone: (306) 966-5233. Fax: (306) 966-4796. E-mail: jad929@mail.usask.ca.

*E-mail: markus.hecker@usask.ca..

Funding

Research was supported through the Canada Research Chair program to M.H. and an NSERC Discovery Grant (Grant # 371854-20) to M.H. J.A.D. was supported through the Vanier Canada Graduate Scholarship.

Notes

The authors declare no competing financial interest.

■ ACKNOWLEDGMENTS

Special thanks to Ron Ek and the team at the Kootenay Trout Hatchery for supplying white sturgeon embryos and to Dr. Bob Freeman at Harvard University for assistance in constructing the reference proteome.

■ REFERENCES

(1) Buckler, J.; Candrl, J. S.; McKee, M. J.; Papoulias, D. M.; Tillitt, D. E.; Galat, D. L. Sensitivity of shovelnose sturgeon (*Scaphirhynchus platorynchus*) and pallid sturgeon (*S. albus*) early life stages to PCB-126 and 2,3,7,8-TCDD exposure. *Environ. Toxicol. Chem.* **2015**, *34* (6), 1417−1424.

(2) Doering, J. A.; Giesy, J. P.; Wiseman, S.; Hecker, M. Predicting the sensitivity of fishes to dioxin-like compounds: possible role of the aryl hydrocarbon receptor (AhR) ligand binding domain. *Environ. Sci. Pollut. Res.* **2013**, *20* (3), 1219−1224.

(3) Elonen, G. E.; Spehar, R. L.; Holcombe, G. W.; Johnson, R. D.; Fernandez, J. D.; Erickson, R. J.; Tietge, J. E.; Cook, P. M. Comparative toxicity of 2,3,7,8-tetrachlorodibenzo-*p*-dioxin to seven freshwater fish species during early life-stage development. *Environ. Toxicol. Chem.* **1998**, *17*, 472−483.

DOI: 10.1021/acs.est.6b00490
Environ. Sci. Technol. 2016, 50, 4826−4835

(4) Johnson, R. D.; Tietge, J. E.; Jensen, K. M.; Fernandez, J. D.; Linnum, A. L.; Lothenbach, D. B.; Holcombe, G. W.; Cook, P. M.; Christ, S. A.; Lattier, D. L.; Gordon, D. A. Toxicity of 2,3,7,8-tetrachlorodibenzo-*p*-dioxin to early life stage brooke trout (*Salvelinus fontinalis*) following parental dietary exposure. *Environ. Toxicol. Chem.* **1998**, *17* (12), 2408−2421.
(5) Park, Y. J.; Lee, M. J.; Kim, H. R.; Chung, K. H.; Oh, S. M. Developmental toxicity of 2,3,7,8-tetrachlorodibenzo-p-dioxin in artificially fertilized crucian carp (Carassius auratus) embryo. *Sci. Total Environ.* **2014**, *491*−*492*, 271−278.
(6) Toomey, B. H.; Bello, S.; Hahn, M. E.; Cantrell, S.; Wright, P.; Tillitt, D.; Di Giulio, R. T. TCDD induces apoptotic cell death and cytochrome P4501A expression in developing *Fundulus heteroclitus* embryos. *Aquat. Toxicol.* **2001**, *53*, 127−138.
(7) Walker, M. K.; Spitsbergen, J. M.; Olson, J. R.; Peterson, R. E. 2,3,7,8-tetrachlorodibenzo-para-dioxin (TCDD) toxicity during early life stage development of lake trout (*Salvelinus namaycush*). *Can. J. Fish. Aquat. Sci.* **1991**, *48*, 875−883.
(8) Yamauchi, M.; Kim, E. Y.; Iwata, H.; Shima, Y.; Tanabe, S. Toxic effects of 2,3,7,8-tetrachlorodibenzo-*p*-dioxin (TCDD) in developing red seabream (*Pagrus major*) embryos: an association of morphological deformities with AHR1, AHR2 and CYP1A expressions. *Aquat. Toxicol.* **2006**, *80*, 166−179.
(9) Zabel, E. W.; Cook, P. M.; Peterson, R. E. Toxic equivalency factors of polychlorinated dibenzo-p-dioxin, dibenzofuran and biphenyl congeners based on early-life stage mortality in rainbow trout (Oncorhynchus mykiss). *Aquat. Toxicol.* **1995**, *31*, 315−328.
(10) King-Heiden, T. C.; Mehta, V.; Xiong, K. M.; Lanham, K. A.; Antkiewicz, D. S.; Ganser, A.; Heideman, W.; Peterson, R. E. Reproductive and developmental toxicity of dioxin in fish. *Mol. Cell. Endocrinol.* **2012**, *354* (1−2), 121−138.
(11) Okey, A. B. An aryl hydrocarbon receptor odyssey to the shores of toxicology: the Deichmann Lecture, International Congress of Toxicology-XI. *Toxicol. Sci.* **2007**, *98*, 5−38.
(12) Kleeman, J. M.; Olson, J. R.; Peterson, R. E. Species differences in 2,3,7,8-tetrachlorodibenzo-p-dioxin toxicity and biotransformation in fish. *Toxicol. Sci.* **1988**, *10* (2), 206−213.
(13) Spitsbergen, J. M.; Schat, K. A.; Kleeman, J. M.; Peterson, R. E. Interactions of 2,3,7,8-tetrachlorodibenzo-p-dioxin (TCDD) with immune responses of rainbow trout. *Vet. Immunol. Immunopathol.* **1986**, *12* (1−4), 263−280.
(14) Walter, G. L.; Jones, P. D.; Giesy, J. P. Pathologic alterations in adult rainbow trout, *Oncorhynchus mykiss*, exposed to dietary 2,3,7,8-tetrachlorodibenzo-p-dioxin. *Aquat. Toxicol.* **2000**, *50*, 287−299.
(15) Giesy, J. P.; Jones, P. D.; Kannan, K.; Newstead, J. L.; Tillitt, D. E.; Williams, L. L. Effects of chronic dietary exposure to environmentally relevant concentrations to 2,3,7,8-tetrachlorodibenzo-*p*-dioxin on survival, growth, reproduction and biochemical responses of female rainbow trout (*Oncorhynchus mykiss*). *Aquat. Toxicol.* **2002**, *59* (1−2), 35−53.
(16) Spitsbergen, J. M.; Kleeman, J. M.; Peterson, R. E. 2,3,7,8-tetrachlorodibenzo-p-dioxin toxicity in yellow perch (*Perca flavescens*). *J. Toxicol. Environ. Health* **1988**, *23*, 359−383.
(17) Spitsbergen, J. M.; Kleeman, J. M.; Peterson, R. E. Morphologic lesions and acute toxicity in rainbow trout (*Salmo gairdneri*) treated with 2,3,7,8-tetrachlorodibenzo-p-dioxin. *J. Toxicol. Environ. Health* **1988**, *23*, 333−358.
(18) Denison, M. S.; Heath-Pagliuso, S. The Ah receptor: a regulator of the biochemical and toxicological actions of structurally diverse chemicals. *Bull. Environ. Contam. Toxicol.* **1998**, *61* (5), 557−568.
(19) Van den Berg, M.; Birnbaum, L.; Bosveld, A. T. C.; Brunstrom, B.; Cook, P.; Feeley, M.; Giesy, J. P.; Hanberg, A.; Hasegawa, R.; Kennedy, S. W.; Kubiak, T.; Larsen, J. C.; van Leeuwen, R. X. R.; Liem, A. K. D.; Nolt, C.; Peterson, R. E.; Poellinger, L.; Safe, S.; Schrenk, D.; Tillitt, D.; Tysklind, M.; Younes, M.; Waern, F.; Zacharewski, T. Toxic equivalency factors (TEFs) for PCBs, PCDDs, PECDFs for human and wildlife. *Enviro. Hlth. Persp.* **1998**, *106*, 775−792.
(20) Billiard, S.; Querbach, K.; Hodson, P. Toxicity of retene to early life stages of two freshwater fish species. *Environ. Toxicol. Chem.* **1999**, *18*, 2070−2077.
(21) Billiard, S. M.; Hahn, M. E.; Franks, D. G.; Peterson, R. E.; Bols, N. C.; Hodson, P. V. Binding of polycyclic aromatic hydrocarbons (PAHs) to teleost aryl hydrocarbon receptors (AHRs). *Comp. Biochem. Physiol., Part B: Biochem. Mol. Biol.* **2002**, *133*, 55−68.
(22) Jayasundara, N.; Van Tiem Garner, L.; Meyer, J. N.; Erwin, K. N.; Di Giulio, R. T. AHR2-mediated transcriptomic responses underlying the synergistic cardiac developmental toxicity of PAHs. *Toxicol. Sci.* **2015**, *143* (2), 469−481.
(23) Van Tiem, L. A.; Di Giulio, R. T. AHR2 knockdown prevents PAH-mediated cardiac toxicity and XRE- and ARE-associated gene induction in zebrafish (*Danio rerio*). *Toxicol. Appl. Pharmacol.* **2011**, *254* (3), 280−287.
(24) Walker, M. K.; Cook, P. M.; Butterworth, B. C.; Zabel, E. W.; Peterson, R. E. Potency of a complex mixture of polychlorinated dibenzo-p-dioxin, dibenzofuran, and biphenyl congeners compared to 2,3,7,8-tetrachlorodibenzo-p-dioxin in causing fish early life stage mortality. *Toxicol. Sci.* **1996**, *30*, 178−186.
(25) Zabel, E. W.; Walker, M. K.; Hornung, M. W.; Clayton, M. K.; Peterson, R. E. Interactions of polychlorinated dibenzo-p-dioxin, dibenzofuran, and biphenyl congeners for producing rainbot trout early life stage mortality. *Toxicol. Appl. Pharmacol.* **1995**, *134*, 204−213.
(26) Doering, J. A.; Wiseman, S.; Beitel, S. C.; Tendler, B. J.; Giesy, J. P.; Hecker, M. Tissue specificity of aryl hydrocarbon receptor (AhR) mediated responses and relative sensitivity of white sturgeon (*Acipenser transmontanus*) to an AhR agonist. *Aquat. Toxicol.* **2012**, *114*−*115*, 125−133.
(27) Doering, J. A.; Farmahin, R.; Wiseman, S.; Kennedy, S.; Giesy, J. P.; Hecker, M. Functionality of aryl hydrocarbon receptors (AhR1 and AhR2) of white sturgeon (Acipenser transmontanus) and implications for the risk assessment of dioxin-like compounds. *Environ. Sci. Technol.* **2014**, *48*, 8219−8226.
(28) Doering, J. A.; Wiseman, S.; Beitel, S. C.; Giesy, J. P.; Hecker, M. Identification and expression of aryl hydrocarbon receptors (AhR1 and AhR2) provide insight in an evolutionary context regarding sensitivity of white sturgeon (*Acipenser transmontanus*) to dioxin-like compounds. *Aquat. Toxicol.* **2014**, *150*, 27−35.
(29) Doering, J. A.; Farmahin, R.; Wiseman, S.; Beitel, S. C.; Kennedy, S. W.; Giesy, J. P.; Hecker, M. Differences in activation of aryl hydrocarbon receptors of white sturgeon relative to lake sturgeon are predicted by identities of key amino acids in the ligand binding domain. *Environ. Sci. Technol.* **2015**, *49*, 4681−4689.
(30) Eisner, B. K.; Doering, J. A.; Beitel, S. C.; Wiseman, S.; Raine, J. C.; Hecker, M. Cross-species comparison of relative potencies and relative sensitivities of fishes to dibenzo-p-dioxins, dibenzofurans, and polychlorinated biphenyls in vitro. *Environ. Toxicol. Chem.* **2016**, *35* (1), 173−181.
(31) Nisbet, I. C. T.; LaGoy, P. K. Toxic equivalency factors (TEFs) for polycyclic aromatic hydrocarbons (PAHs). *Regul. Toxicol. Pharmacol.* **1992**, *16*, 290−300.
(32) Neilson, A. H. *PAHs and related compounds. Biology*; Springer: Berlin, Germany, 1998.
(33) Spitsbergen, J. M.; Kleeman, J. M.; Peterson, R. E. Morphologic lesions and acute toxicity in rainbow trout (*Salmo gairdneri*) treated with 2,3,7,8-tetrachlorobibenzo-*p*-dioxin. *J. Toxicol. Environ. Health* **1988**, *23* (3), 333−358.
(34) Vizcaino, J. A.; Deutsch, E. W.; Wang, R.; Csordas, A.; Reisinger, F.; Rios, D.; Dianes, J. A.; Sun, Z.; Farrah, T.; Bandeira, N.; Binz, P. A.; Xenarios, I.; Eisenacher, M.; Mayer, G.; Gatto, L.; Campos, A.; Chalkley, R. J.; Kraus, H. J.; Albar, J. P.; Martinez-Bartolome, S.; Apweiler, R.; Omenn, G. S.; Martens, L.; Jones, A. R.; Hermjakob, H. ProteomeXchanger provides globally coordinated proteomics data submission and dissemination. *Nat. Biotechnol.* **2014**, *32* (3), 223−226.
(35) Wuhr, M.; Freeman, R. M., Jr.; Presler, M.; Horb, M. E.; Peshkin, L.; Gygi, S. P.; Kirschner, M. W. Deep proteomics of the Xenopus laevis egg using an mRNA-derived reference database. *Curr. Biol.* **2014**, *24* (13), 1467−1475.

DOI: 10.1021/acs.est.6b00490
Environ. Sci. Technol. 2016, 50, 4826−4835

(36) Dray, S.; Chessel, D.; Thioulouse, J. Co-inertia analysis and the linking of ecological data tables. *Ecology* **2003**, *84*, 3078−3089.
(37) Bindea, G.; Mlecnik, B.; Hackl, H.; Charoentong, P.; Tosolini, M.; Kirilovsky, A.; Fridman, W. H.; Pages, F.; Trajanoski, Z.; Galon, J. ClueGO: a Cytoscape plug-in to decipher functionally grouped gene ontology and pathway annotation networks. *Bioinformatics* **2009**, *25* (8), 1091−1093.
(38) Shannon, P.; Markiel, A.; Ozier, O.; Baliga, N. S.; Wang, J. T.; Ramage, D.; Amin, N.; Schwikowski, B.; Ideker, T. Cytoscape: a software environment for integrated models of biomolecular interaction networks. *Genome Res.* **2003**, *13* (11), 2498−2504.
(39) Hahn, M. E. Aryl hydrocarbon receptors: diversity and evolution. *Chem.-Biol. Interact.* **2002**, *141*, 131−160.
(40) Alexeyenko, A.; Wassenberg, D. M.; Lobenhofer, E. K.; Yen, J.; Linney, E.; Sonnhammer, E. L. L.; Meyer, J. N. Dynamic zebrafish interactome reveals transcriptional mechanisms of dioxin toxicity. *PLoS One* **2010**, *5* (5), e10465.
(41) Li, Z.; Xu, H.; Zheng, W.; Lam, S. H.; Gong, Z. RNA-sequencing analysis of TCDD-induced responses in zebrafish liver reveals high relatedness to in vivo mammalian models and conserved biological pathways. *PLoS One* **2013**, *8* (10), e77292.
(42) Whitehead, A.; Triant, D. A.; Champlin, D.; Nacci, D. Comparative transcriptomics implicates mechanisms of evolved pollution tolerance in a killifish population. *Mol. Ecol.* **2010**, *19*, 5186−5203.
(43) Brinkmann, M.; Koglin, S.; Eisner, B.; Wiseman, S.; Hecker, M.; Eichbaum, K.; Thalmann, B.; Buchinger, S.; Reifferscheid, G.; Hollert, H. Characterization of transcriptional responses to dioxins and dioxin-like contaminants in roach (Rutilus rutilus) using whole transcriptome analysis. *Sci. Total Environ.* **2016**, *541*, 412−423.
(44) Huang, L.; Zuo, Z.; Zhang, Y.; Wu, M.; Lin, J. J.; Wang, C. Use of toxicogenomics to predict the potential toxic effects of benzo(a)pyrene on zebrafish embryos: Ocular developmental toxicity. *Chemosphere* **2014**, *108*, 55−61.
(45) Boutros, P. C.; Yan, R.; Moffat, I. D.; Pohjanvirta, R.; Okey, A. B. Transcriptomic responses to 2,3,7,8-tetrachlorodibenzo-p-dioxin (TCDD) in liver: Comparison of rat and mouse. *BMC Genomics* **2008**, *9*, 419.
(46) Kopec, A. K.; Burgoon, L. D.; Ibrahim-Aibo, D.; Burg, A. R.; Lee, A. W.; Tashiro, C.; Potter, D.; Sharratt, B.; Harkema, J. R.; Rowlands, J. C.; Budinsky, R. A.; Zacharewski, T. R. Automated dose-response analysis and comparative toxicogenomic evaluation of the hepatic effects elicited by TCDD, TCDF, and PCB126 in C57BL/6 mice. *Toxicol. Sci.* **2010**, *118* (1), 286−297.
(47) Juschke, C.; Dohnal, I.; Pichler, P.; Harzer, H.; Swart, R.; Ammerer, G.; Mechtler, K.; Knoblicj, J. A. Transcriptome and proteome quantification of a tumor model provides novel insights into post-translational gene regulation. *Genome Biol.* **2013**, *14*, r133.
(48) Tomanek, L. Environmental proteomics: changes in the proteome of marine organisms in response to environmental stress, pollutants, infection, symbiosis, and development. *Annu. Rev. Mar. Sci.* **2011**, *3*, 373−399.
(49) Garner, L. V.; Di Giulio, R. T. Glutathione transferase pi class 2 (GSTp2) protects against the cardiac deformities caused by exposure to PAHs but not PCB-126 in zebrafish embryos. *Comp. Biochem. Physiol., Part C: Toxicol. Pharmacol.* **2012**, *155*, 573−579.
(50) Timme-Laragy, A. R.; Cockman, C. J.; Matson, C. W.; Di Giulio, R. T. Synergistic induction of AHR regulated genes in developmental toxicity from co-exposure to two model PAHs in zebrafish. *Aquat. Toxicol.* **2007**, *85*, 241−250.
(51) Timme-Laragy, A. R.; Van Tiem, L. A.; Linney, E. A.; Di Giulio, R. T. Antioxidant responses and NRF2 in synergistic development toxicity of PAHs in zebrafish. *Toxicol. Sci.* **2009**, *109*, 217−227.
(52) Dalton, T. P.; Puga, A.; Shertzer, H. G. Induction of cellular oxidative stress by aryl hydrocarbon receptor activation. *Chem.-Biol. Interact.* **2002**, *141*, 77−95.
(53) Carney, S. A.; Peterson, R. E.; Heideman, W. 2,3,7,8-tetrachlorodibenzo-p-dioxin activation of the aryl hydrocarbon receptor/aryl hydrocarbon receptor nuclear translocator pathway causes developmental toxicity through a CYP1A-independent mechanism in zebrafish. *Mol. Pharmacol.* **2004**, *66*, 512−521.
(54) Lammi, L.; Arte, S.; Somer, M.; Jarvinen, H.; Lahermo, P.; Thesleff, I.; Pirinen, S.; Nieminen, P. Mutations in AXIN2 cause familial tooth agenesis and predispose to colorectal cancer. *Am. J. Hum. Genet.* **2004**, *74*, 1043−1050.
(55) Logan, C. Y.; Nusse, R. The wnt signaling pathway in development and disease. *Annu. Rev. Cell Dev. Biol.* **2004**, *20*, 781−810.
(56) Mathew, L. K.; Simonich, M. T.; Tanguay, R. L. AHR-dependent misregulation of Wnt signaling disrupts tissue regeneration. *Biochem. Pharmacol.* **2009**, *77*, 498−507.
(57) Teraoka, H.; Dong, W.; Okuhara, Y.; Iwasa, H.; Shindo, A.; Hill, A. J.; Kawakami, A.; Hiraga, T. Impairment of lower jaw growth in developing zebrafish exposed to 2,3,7,8-tetrachlorodibenzo-p-dioxin and reduced hedgehog expression. *Aquat. Toxicol.* **2006**, *78*, 103−113.
(58) Andreasen, E. A.; Mathew, L. K.; Lohr, C. V.; Hasson, R.; Tanguay, R. L. Aryl hydrocarbon receptor activation impairs extracellular matrix remodeling during zebra fish fin regeneration. *Toxicol. Sci.* **2007**, *95* (1), 215−226.
(59) Planchart, A.; Mattingly, C. J. 2,3,7,8-tetrachlorodibenzo-p-dioxin upregulated FoxQ1b in zebrafish jaw primordium. *Chem. Res. Toxicol.* **2010**, *23* (3), 480−487.
(60) Carney, S. A.; Chen, J.; Burns, C. G.; Xiong, K. M.; Peterson, R. E.; Heideman, W. Aryl hydrocarbon receptor activation produces heart-specific transcriptional and toxic responses in developing zebrafish. *Mol. Pharmcol.* **2006**, *70* (2), 549−561.
(61) Mehta, V.; Peterson, R. E.; Heideman, W. 2,3,7,8-tetrachlorodibenzo-p-dioxin exposure prevents cardiac valve formation in developing zebrafish. *Toxicol. Sci.* **2008**, *104* (2), 303−311.
(62) Teraoka, H.; Kubota, A.; Dong, W.; Kawai, Y.; Yamazaki, K.; Mori, C.; Harada, Y.; Peterson, R. E.; Hiraga, T. Role of the cyclooxygenase 2-thromboxane pathway in 2,3,7,8-tetrachlorodibenzo-p-dioxin-induced decrease in mesencephalic vein blood flow in the zebrafish embryo. *Toxicol. Appl. Pharmacol.* **2009**, *234*, 33−40.
(63) Mellor, C. L.; Steinmetz, F. P.; Cronin, M. T. D. The identification of nuclear receptors associated with hepatic steatosis to develop and extend adverse outcome pathways. *Crit. Rev. Toxicol.* **2016**, *46*, 138.
(64) Shou, M.; Gonzalez, F. J.; Gelboin, H. V. Stereoselective epoxidation and hydration at the K-region of polycyclic aromatic hydrocarbons by cDNA-expressed cytochromes P450 1A1, 1A2, and epoxide hydrolase. *Biochemistry* **1996**, *35* (49), 15807−15813.
(65) Liu, F.; Wiseman, S.; Wan, Y.; Doering, J. A.; Hecker, M.; Lam, M. H. W.; Giesy, J. P. Multi-species comparison of the mechanism of biotransformation of MeO-BDEs to OH-BDEs in fish. *Aquat. Toxicol.* **2012**, *114-115*, 182−188.
(66) Villeneuve, D. L.; Crump, D.; Garcia-Reyero, N.; Hecker, M.; Hutchinson, T. H.; LaLone, C. A.; Landesmann, B.; Lettieri, T.; Munn, S.; Nepelska, M.; Ottinger, M. A.; Vergauwen, L.; Whelan, M. Adverse outcome pathway (AOP) development I: Strategies and principles. *Toxicol. Sci.* **2014**, *142* (2), 312−320.
(67) Ankley, G. T.; Bennett, R. S.; Erickson, R. J.; Hoff, D. J.; Hornung, M. W.; Johnson, R. D.; Mount, D. R.; Nichols, J. W.; Russom, C. L.; Schmieder, P. K.; Serrano, J. A.; Tietge, J. E.; Villeneuve, D. L. Adverse outcome pathways: A conceptual framework to support ecotoxicology research and risk assessment. *Environ. Toxicol. Chem.* **2010**, *29* (3), 730−741.

DOI: 10.1021/acs.est.6b00490
Environ. Sci. Technol. 2016, 50, 4826−4835

Supporting Information

High conservation in transcriptomic and proteomic response of white sturgeon to equipotent concentrations of 2,3,7,8-TCDD, PCB 77, and benzo[a]pyrene

Jon A. Doering,*[,†,‡] Song Tang,[§] Hui Peng,[‡] Bryanna K. Eisner,[‡] Jianxian Sun,[‡] John P. Giesy,[‡,∥] Steve Wiseman,[‡] Markus Hecker*[,‡,§]

[†] Toxicology Graduate Program, University of Saskatchewan, Saskatoon, SK, Canada

[‡] Toxicology Centre, University of Saskatchewan, Saskatoon, SK, Canada

[§] School of Environment and Sustainability, University of Saskatchewan, Saskatoon, SK, Canada

[∥] Department of Veterinary Biomedical Sciences, University of Saskatchewan, Saskatoon, SK, Canada

*To whom correspondence should be addressed at University of Saskatchewan, Toxicology Centre, 44 Campus Drive, Saskatoon, SK, Canada, S7N 5B3. Phone: (306) 966-5233. Fax: (306) 966-4796. E-mail: jad929@mail.usask.ca

*markus.hecker@usask.ca.

Summary

MATERIALS AND METHODS

Transcriptomics

Total RNA was extracted from approximately 30mg of liver from each individual by use of the RNeasy Lipid Tissue Mini Kit (Qiagen, Mississauga, ON). Concentrations of RNA were determined by use of a NanoDrop ND-1000 Spectrophotometer (Nanodrop Technologies, Welmington, DE). Quality of RNA was determined through RNA Integrity Number (RIN) by use of a 2100 Bioanalyzer (Agilent, Clara, CA). Only samples with an RIN ≥8 were used in subsequent analysis (Control n=3; TCDD, PCB 77, and BaP n=4). Equal amounts of RNA from each individual were pooled to create one sample of 2μg RNA per treatment. One RNA-Seq library per treatment was prepared by use of the Tru-Seq RNA Sample Prep Kit (*Illumina*, San Diego, CA). Quality of libraries was confirmed by use of a 2100 Bioanalyzer (Agilent). Each library was loaded onto a separate Mi-Seq v3 150 cycle cartridge (*Illumina*) and run as 75 base-pair (bp) paired-end reads on a Mi-Seq sequencer (*Illumina*) at the Toxicology Centre (University of Saskatchewan, Saskatoon, SK). Raw sequences have been made available in the National Center for Biotechnology Information (NCBI) Gene Expression Omnibus (GEO) (Accession #GSE79624).

No public databases for either the genome or transcriptome of white sturgeon were available. Therefore, a comprehensive reference transcriptome was constructed by use of *de novo* assembly from reads for liver of white sturgeon described here and in earlier studies described elsewhere.[1] The reference transcriptome has been made available in the NCBI GEO (Accession #GSE79624). Specifically, a total of six Mi-Seq (*Illumina*) runs at 75bp paired-end reads and four Hi-Seq (*Illumina*) runs on individual lanes at 100bp paired-end reads were used.[28] Prior to

assembly, the quality of raw reads was assessed using FASTQC (http://www.bioinformatics.babraham.ac.uk/projects/fastqc/) and the terminal 5' and 3' nucleotides were trimmed from all sequences to ensure high qualities (Phred quality score ≥30). All subsequent analyses were based on these cleaned reads. A merging step was then carried out on the paired reads from each of these four samples so that any overlapping reads were merged into a single read. Contigs (continuous, overlapping sequences assembled from individual sequencing reads) for the reference transcriptome were *de novo* assembled from the merged reads and unmerged paired-end reads from individual sequencing reads by use of CLC genomics workbench v.5.0 (CLC Bio, Aarhus, Denmark) with default parameters. The minimum contig length was set to 200bp and this assembly process generated 69 312 unique contigs. The mean contig size was 1 060bp. Contigs comprising the reference transcriptome were annotated by use of BlastX searches in Blast2GO v.2.5.0 software[2] with a minimum *E*-value of $<10^{-6}$ against sequences in the NCBI non-redundant protein database for zebrafish.

Both merged and unmerged reads comprising each treatment were aligned to the reference transcriptome. The total numbers of paired-end reads were 21 113 596, 20 913 356, 21 935 312, and 19 015 255 for the control, TCDD, PCB 77, and BaP treatments, respectively. Mapped reads were filtered based on a count per million (CPM) of >5 in at least one of the four treatments and normalized by use of the 'edgeR' package[3] in R software v.3.1.2 (R Foundation for Statistical Computing, Vienna, Austria). Fold-changes for each contig for each treatment were calculated based on CPM relative to CPM in the control. Value of variation of biological variation (BCV) was set to 0.2 and significance of differentially expressed contigs was scored by a cutoff false discovery rate (FDR) of 0.05. Since statistical analysis cannot be conducted on the

pooled libraries, significance of differentially expressed transcripts was scored by a change in abundance greater than or equal to a threshold of ±2-fold relative to controls. Quantitative real-time polymerase chain reaction (qRT-PCR) was used to confirm results of transcriptome analysis and assess variance among pooled individuals for a subset of six genes as described previously.[1,4,5] qRT-PCR primers for amplification of genes of interest were designed by use of Primer3 software[6] based on sequences from the white sturgeon liver transcriptome described here or were based on primers of white sturgeon published previously (Table S1).[4] Abundance of transcripts was quantified by normalizing to β-actin according to methods described previously.[7]

Proteomics

Livers from individuals of each treatment group were pooled at equal mass to create one sample per treatment (Control n=3; TCDD, PCB 77, and BaP n=4). Pooled livers were homogenized on ice in a lysis buffer (20mM HEPES, 1.5mM $MgCl_2$, 0.2mM EDTA, 100mM KCl, 420mM NaCl, 20% Glycerol, and protease inhibitor cocktail, pH 7.4) by use of a model 100 Sonic Dismembrator (Thermo Fisher Scientific, Waltham, MA). Liver lysates were centrifuged at 15 000×g for 15min at 4°C and soluble supernatant was transferred to a new tube and centrifuged again as a final clearing step. Total concentrations of protein in the supernatant were determined by use of the Bradford assay[8], with a bovine serum albumin (BSA) standard. Filter-aided sample preparation was used for digestion of proteins by use of spin ultrafiltration filters with a molecular weight cut off of 30 000 daltons (30kDa). Aliquots of the lysates containing approximately 100µg of protein were transferred to YM-30 microcon filter units (Millipore, Burlington, ON) and centrifuged at 14 000xg for 30min. Salt and other interferences in the buffer were removed from samples by washing three times with 0.1M Tris-HCl. Samples

were reduced for 60min at 37°C with 50µL of 5mM DTT, and then carboxymethylated in the dark at room temperature for 30min with 15mM iodoacetamide. Samples were further digested overnight with 5µg trypsin at 20:1 protein to trypsin and with gentle shaking. Digestion was terminated by adding formic acid to 1% (v/v). The final sample was collected by centrifugation at 14 000xg for 30min. Samples were stored at -80°C until analyzed.

Each sample was loaded in duplicate onto a 75mm inner diameter fused silica microcapillary column (Polymicron Technologies, Phoenix, AZ) packed with 10cm of Luna 3-mC18 100Å reversed phase particles (Phenomenex, Torrance, CA) and placed in-line with a nanoLC-electrospray ion source (Proxeon, Mississauga, ON) interfaced to an LTQ Orbitrap Velos hybrid mass spectrometer (Thermo Fisher Scientific) at the University of Toronto (Toronto, ON). The organic gradient was driven by the EASY-nLC system at 300nL/min. The mobile phase consisted of 95% acetonitrile with 0.1% formic acid (A) and 5% acetonitrile (B). B at 2% was increased to 6% after 2min, 62mins later B was increased to 24%, 26min later B was increased to 90% and held static for 5min, and then decreased to initial conditions of 2% of B and held for 8min for equilibration. Positive precursor ions (400-2 000m/z) were subjected to data-dependent collision-induced dissociation as the instrument cycled through one full mass scan at 60 000 full-width at half maximum followed by 17 successive MS/MS scans targeting the most intense precursors with dynamic exclusion and +2/+3 charge state selection enabled. Raw MS/MS sequences have been deposited to the ProteomeXchange Consortium via the Proteomics Identifications (PRIDE) partner repository (Accession #PXD003840).[9]

No public databases for proteome sequences of white sturgeon were available. Therefore, a comprehensive, genome-free, artifact-free reference proteome was constructed based on the liver transcriptome of white sturgeon through the online pipeline at http://kirschner.med.harvard.edu/tools/mz_ref_db.html.[10] The reference proteome has been made available in the PRIDE partner repository (Accession #PXD003840). Raw MS/MS files were analyzed by use of MaxQuant v.1.5.1.2.[11] MS/MS spectra were searched against the reference proteome containing forward and reversed (decoy) sequences, allowing for variable modifications of methionine oxidation and N-terminal acetylation and fixed cysteine carbamidomethylation. Parent mass and fragment ions were matched by use of a maximal initial mass deviation of 7p.p.m and 0.5Th, respectively. Protein FDR was set to 0.01. Spectral count was used for label-free quantification of the proteins, and only proteins with spectral counts greater than four were used in further analyses. Sequences comprising each treatment were aligned to the reference proteome. Since statistical analysis cannot be conducted on the pooled samples, significance of differentially expressed proteins was scored by a change in abundance greater than or equal to a threshold of ±2-fold relative to controls.

Data Analysis

Venn plots were produced by use of the VennDiagram package with R software.[12] Density ternary plots were produced by use of the ggtern package (ggtern.com) with R software. Only transcripts and proteins that had changes in abundance greater than or equal to a threshold of ±2-fold were used in venn plots and ternary plots. Coinertia analysis (CIA) was performed by use of the ade4 and ggplot2 (http://ggplot2.org) packages with R software.[13] Accession numbers for each altered protein were converted to mRNA accession numbers from zebrafish prior to

pathway analysis by use of the database to database (db2db) tool in bioDBnet (http://biodbnet.abcc.ncifcrf.gov/db/db2db.php). Only transcripts and proteins that had changes in abundance greater than or equal to a threshold of ±2-fold were used in pathway analysis. Linear regression was performed by use of GraphPad Prism version 6.0 (San Diego, CA).

Table S1 Sequences, annealing temperatures, primer efficiencies, and corresponding gene Genbank accession numbers of oligonucleotide primers used in quantitative real-time polymerase chain reaction (qRT-PCR).

Target Gene	Accession #	Primer Sequence (5'-3')	Efficiency (%)	Annealing Temp (°C)
β-actin[a]	FJ205611	Forward: CCGAGCACAATGAAAATCAA Reverse: ACATCTGCTGGAAGGTGGAC	96	60
CYP1A[a]	JQ660369	Forward: GATCCCTCCACCTTCTCTCC Reverse: GCCGATAGACTCACCAATGC	99	60
AHRR	NA	Forward: GATGCACCAGAATGTGTTCG Reverse: ATGGACCAGTGGAGCTGTGT	107	60
SOD	NA	Forward: GCAGGTCCGTGGTGATTCAT Reverse: TTCCGATGACACAGCAAGCT	87	60
FBP1A	NA	Forward: CAATGGTGGCTGATGTTCAC Reverse: GTGGATGCACTCTGGCTGTA	102	60
SOX9	NA	Forward: AAGGGCTATGACTGGACCCT Reverse: GTGAAGATGCGGGTACTGGT	100	60
CYP7A1A	NA	Forward: GCCATTGAAACCTCAAGGAA Reverse: AGTCCTTCTGTGGTCCATGC	103	60

[a]Adapted from previously published results.[4]

Table S2 Comparison of fold-changes for abundance of transcripts by use of transcriptome sequencing (A) and by use of quantitative real-time polymerase chain reaction (qRT-PCR) (B) in livers of white sturgeon three days following intraperitoneal injection with 5µg TCDD/kg-bm, 5mg PCB 77/kg-bm, or 30mg BaP/kg-bm.[a]

	A Transcriptomics			B qRT-PCR		
Gene	TCDD	PCB 77	BaP	TCDD	PCB 77	BaP
CYP1A	33-fold	42-fold	50-fold	25-fold ±4	15-fold ±3	24-fold ±8
AHRR	78-fold	105-fold	110-fold	196-fold ±40	103-fold ±22	210-fold ±44
SOD	1.3-fold	1.1-fold	1.5-fold	1.1-fold ±0.1	0.89-fold ±0.3	1.2-fold ±0.5
FBP1A	1.1-fold	1.2-fold	0.83-fold	0.52-fold ±0.1	0.64-fold ±0.4	0.48-fold ±0.2
SOX9	0.21-fold	0.13-fold	0.39-fold	0.28-fold ±0.04	0.22-fold ±0.05	0.59-fold ±0.08
CYP7A1A	0.12-fold	0.44-fold	0.85-fold	0.34-fold ±0.1	0.28-fold ±0.04	0.43-fold ±0.09

[a]Transcriptomics data represented as the mean fold-change where multiple contigs had the same sequence description. qRT-PCR data represented as mean±standard error of the mean (S.E.M.).

Table S3 Comparison of the standard deviation (SD) in abundance of transcripts in livers from the control treatment (n=3) assessed by use of quantitative real-time polymerase chain reaction (qRT-PCR).[a]

Gene	SD
CYP1A	±0.33
AHRR	±0.36
SOD	±0.41
FBP1A	±0.77
SOX9	±0.25
CYP7A1A	±0.36
Average	±0.41

[a]SDs are based on a normalized control value of 1.

Table S4 Number of genes up- or down-regulated by ≥2-fold in the transcriptome and proteome in livers of white sturgeon following exposure to TCDD, PCB 77, or BaP.

Transcriptome		Up-regulated	Down-regulated
	TCDD	378	296
	PCB 77	493	325
	BaP	529	394
Proteome		Up-regulated	Down-regulated
	TCDD	180	102
	PCB 77	270	89
	BaP	218	89

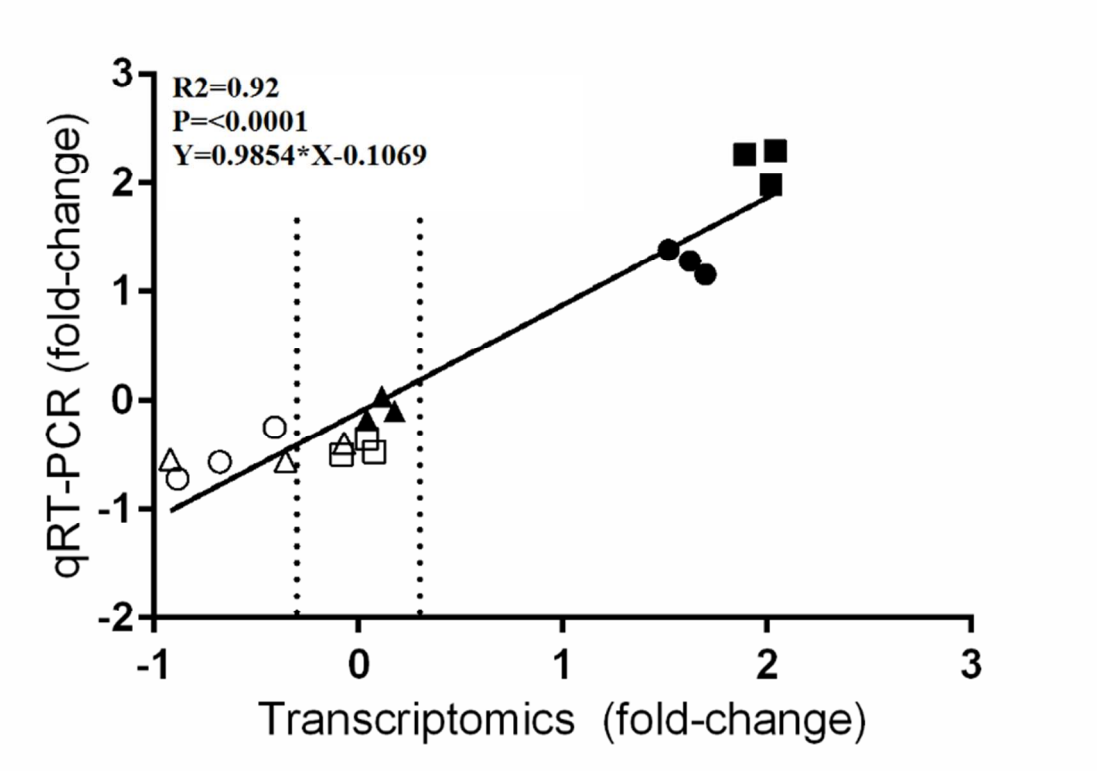

Figure S1 Linear regression of fold-change in abundance of transcripts in livers of white sturgeon exposed to TCDD, PCB 77, or BaP relative to abundance in controls assessed by either quantitative real-time polymerase chain reaction (qRT-PCR) or transcriptome analysis by use of *Illumina* Mi-Seq. Plotted data represents the mean (n=4) for CYP1A (solid circle), AHRR (solid square), SOD (solid triangle), FBP1A (open square), SOX9 (open circle), CYP7A1A (open triangle). Plotted data has been $\log_{10}$ transformed. Plotted data is presented elsewhere (Table S2). Dotted lines indicate the threshold of 2-fold down-regulated and 2-fold up-regulated.

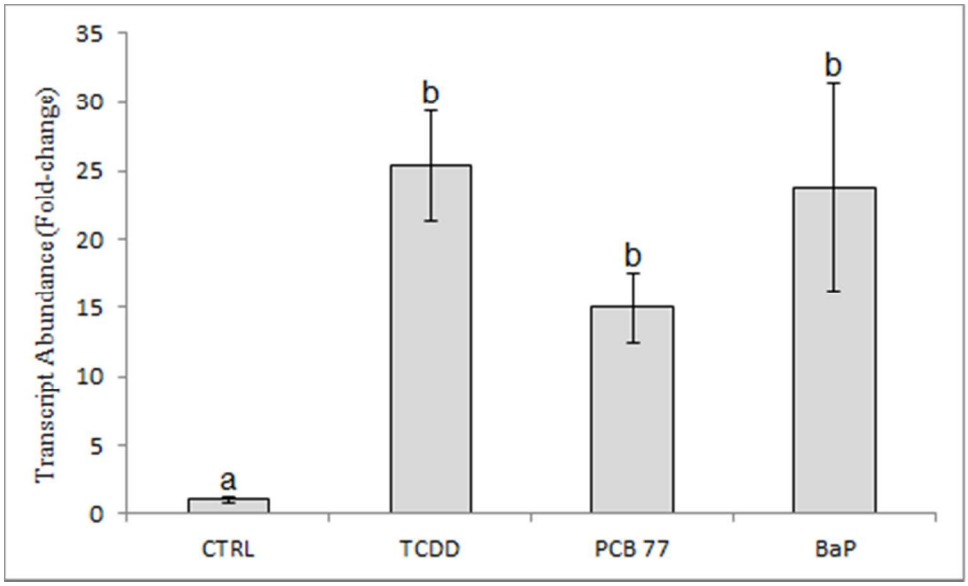

Figure S2 Abundance of transcripts of cytochrome P450 1A (CYP1A) in livers of white sturgeon three days following intraperitoneal injection with either corn oil alone, or corn oil with 5µg TCDD/kg-bm, 5mg PCB 77/kg-bm, or 30mg BaP/kg-bm. Data represent mean±standard error of the mean (S.E.M.). Different letters represent statistical difference by use of analysis of variance (ANOVA) followed by Tukey's post-hoc test ($p \leq 0.05$).

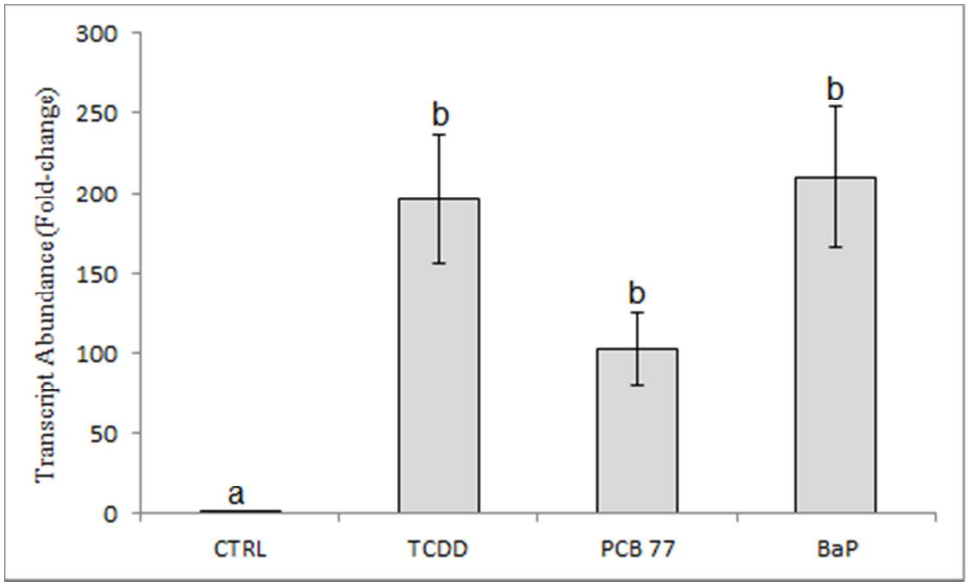

Figure S3 Abundance of transcripts of aryl hydrocarbon receptor repressor (AHRR) in livers of white sturgeon three days following intraperitoneal injection with either corn oil alone, or corn oil with 5µg TCDD/kg-bm, 5mg PCB 77/kg-bm, or 30mg BaP/kg-bm. Data represent mean ± standard error of the mean (S.E.M.). Different letters represent statistical difference by use of analysis of variance (ANOVA) followed by Tukey's post-hoc test ($p \leq 0.05$).

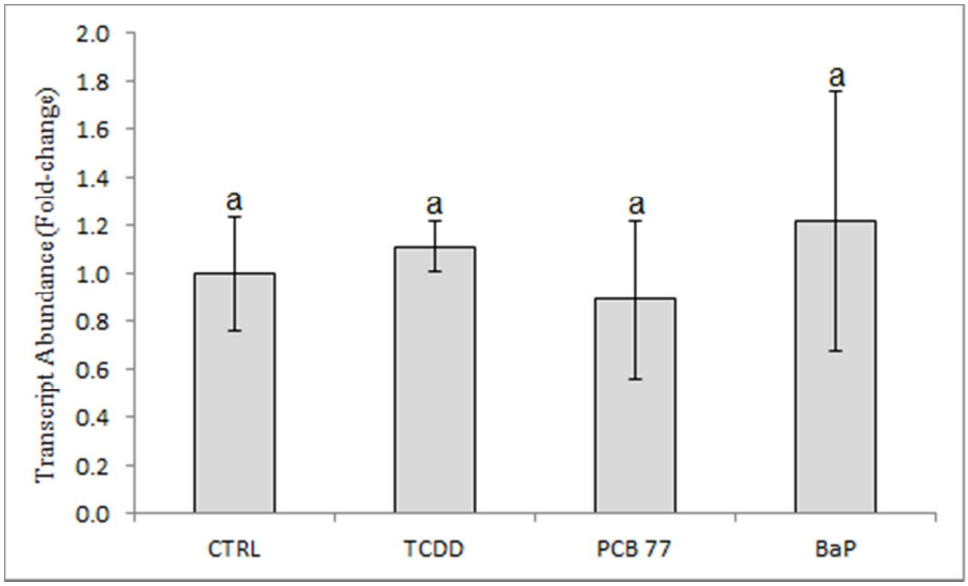

Figure S4 Abundance of transcripts of superoxide dismutase (SOD) in livers of white sturgeon three days following intraperitoneal injection with either corn oil alone, or corn oil with 5µg TCDD/kg-bm, 5mg PCB 77/kg-bm, or 30mg BaP/kg-bm. Data represent mean ± standard error of the mean (S.E.M.). Different letters represent statistical difference by use of analysis of variance (ANOVA) followed by Tukey's post-hoc test ($p \leq 0.05$).

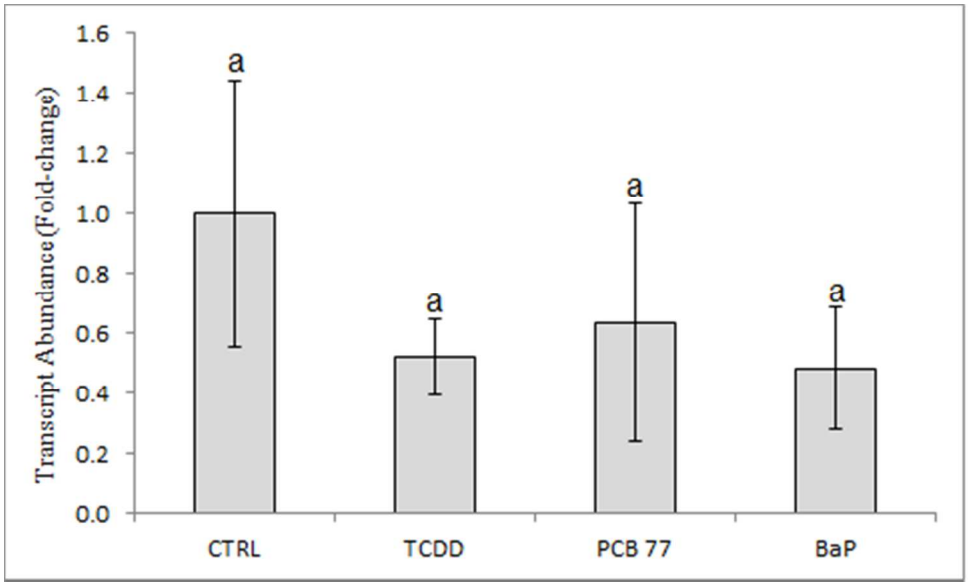

Figure S5 Abundance of transcripts of fructose-1,6-bisphosphatase 1a (FBP1A) in livers of white sturgeon three days following intraperitoneal injection with either corn oil alone, or corn oil with 5µg TCDD/kg-bm, 5mg PCB 77/kg-bm, or 30mg BaP/kg-bm. Data represent mean ± standard error of the mean (S.E.M.). Different letters represent statistical difference by use of analysis of variance (ANOVA) followed by Tukey's post-hoc test ($p \leq 0.05$).

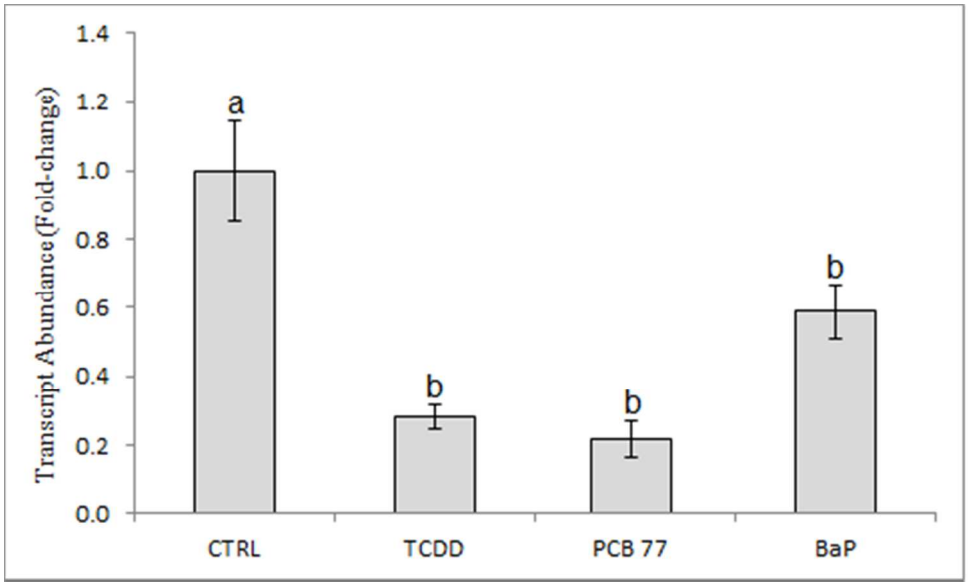

Figure S6 Abundance of transcripts of sex determining region Y-box 9 (SOX9) in livers of white sturgeon three days following intraperitoneal injection with either corn oil alone, or corn oil with 5µg TCDD/kg-bm, 5mg PCB 77/kg-bm, or 30mg BaP/kg-bm. Data represent mean ± standard error of the mean (S.E.M.). Different letters represent statistical difference by use of analysis of variance (ANOVA) followed by Tukey's post-hoc test ($p \leq 0.05$).

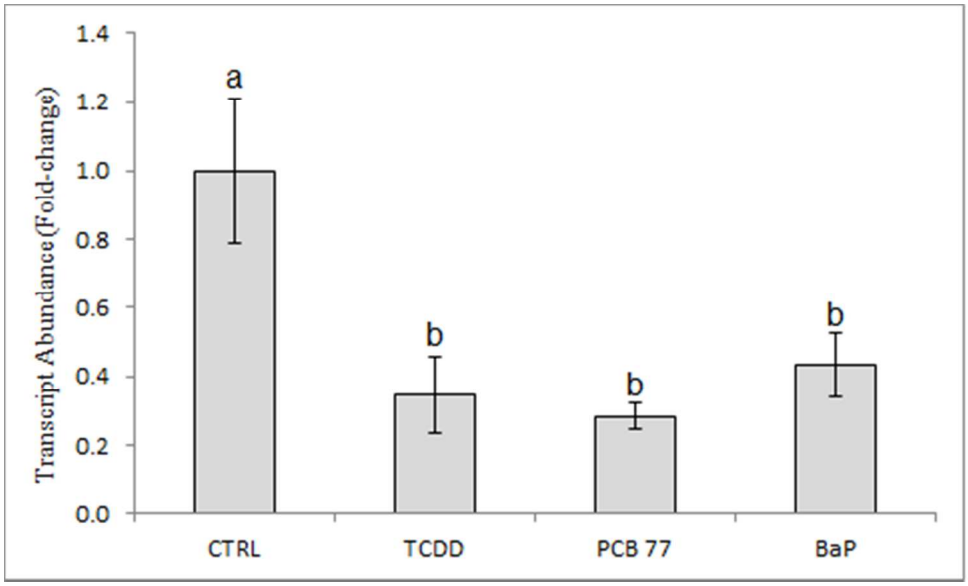

Figure S7 Abundance of transcripts of cholesterol 7-alpha-monooxygenase 1a (CYP7A1A) in livers of white sturgeon three days following intraperitoneal injection with either corn oil alone, or corn oil with 5µg TCDD/kg-bm, 5mg PCB 77/kg-bm, or 30mg BaP/kg-bm. Data represent mean ± standard error of the mean (S.E.M.). Different letters represent statistical difference by use of analysis of variance (ANOVA) followed by Tukey's post-hoc test ($p \leq 0.05$).

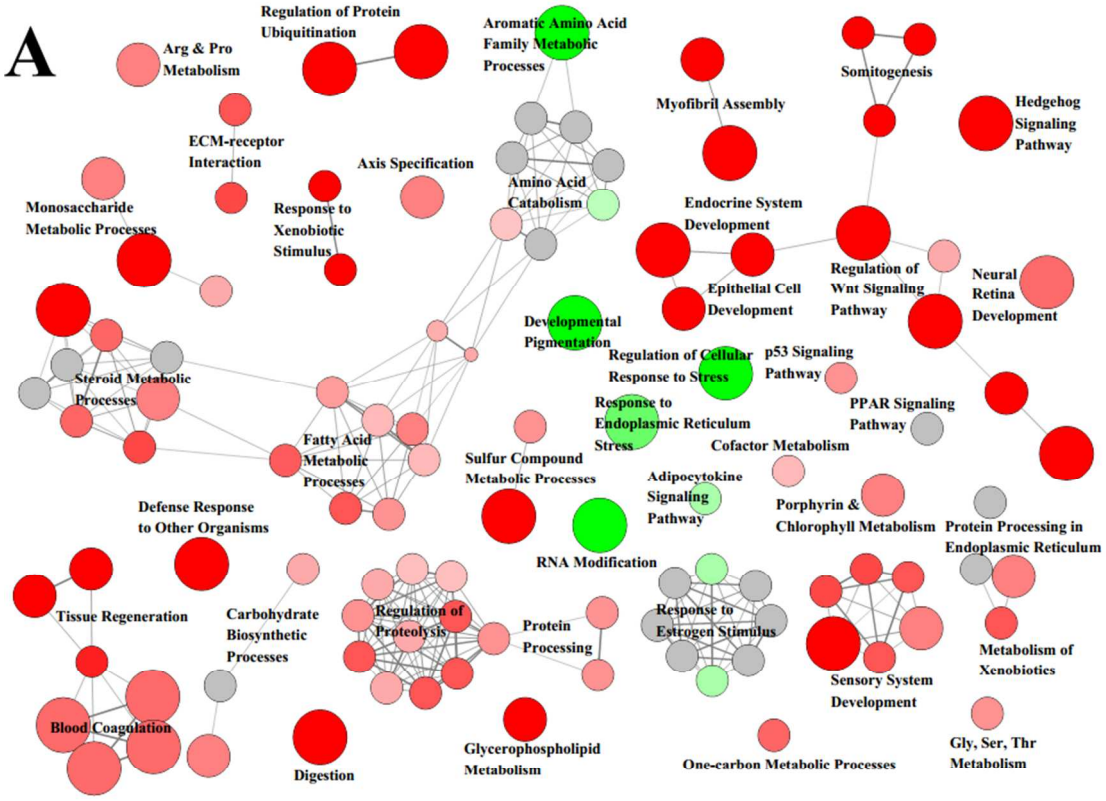
A
Regulation of Protein Ubiquitination
Arg & Pro Metabolism
Aromatic Amino Acid Family Metabolic Processes
Somitogenesis
Myofibril Assembly
Hedgehog Signaling Pathway
ECM-receptor Interaction
Axis Specification
Amino Acid Catabolism
Monosaccharide Metabolic Processes
Response to Xenobiotic Stimulus
Endocrine System Development
Regulation of Wnt Signaling Pathway
Neural Retina Development
Epithelial Cell Development
Developmental Pigmentation
Regulation of Cellular Response to Stress
p53 Signaling Pathway
Steroid Metabolic Processes
Response to Endoplasmic Reticulum Stress
PPAR Signaling Pathway
Fatty Acid Metabolic Processes
Cofactor Metabolism
Sulfur Compound Metabolic Processes
Adipocytokine Signaling Pathway
Porphyrin & Chlorophyll Metabolism
Protein Processing in Endoplasmic Reticulum
Defense Response to Other Organisms
RNA Modification
Tissue Regeneration
Carbohydrate Biosynthetic Processes
Regulation of Proteolysis
Protein Processing
Response to Estrogen Stimulus
Sensory System Development
Metabolism of Xenobiotics
Blood Coagulation
Digestion
Glycerophospholipid Metabolism
One-carbon Metabolic Processes
Gly, Ser, Thr Metabolism
B
Val, Leu, Ile Degradation
Lipid Catabolic Processes
Catabolic Processes
Peroxisome
Pyruvate Metabolism
PPAR Signaling Pathway
Tyr Metabolism
Pentose & Glucuronate Interconversion
Proteasome
Carbohydrate Catabolic Processes
His Metabolism
Amino Acid Metabolism & Biosynthesis
Pentose Phosphate Pathway
Metabolism of Xenobiotics
Ascorbate & Aldarate Metabolism
Glycolysis & Gluconeogenesis
Trp Metabolism
Protein Folding
Response to Hypoxia
Rab Protein Signal Transduction
Gly, Ser, Thr Metabolism
Ribosome Assembly
Nuclear Transport
Translation
Nucleoside Metabolic Processes
NADP Metabolic Processes
Ribosome
ATP Metabolic Processes

Figure S8 Cytoscape visualization of ClueGO clustering results of physiological processes altered by TCDD at the level of the transcriptome (A) and proteome (B) in liver of white sturgeon. Clusters with a greater proportion of up-regulated processes are shown in (red) while clusters with a greater proportion of down-regulated processes are shown in (green). Degree of red or green shows relative abundance of up-regulated vs down-regulated processes in each cluster. Grey clusters consist of 50% up-regulated processes and 50% down-regulated processes. Size of cluster represents the relative number of processes in the cluster. Interconnection between pathways is represented by grey interconnecting lines indicating that these categories share transcript(s) or protein(s).

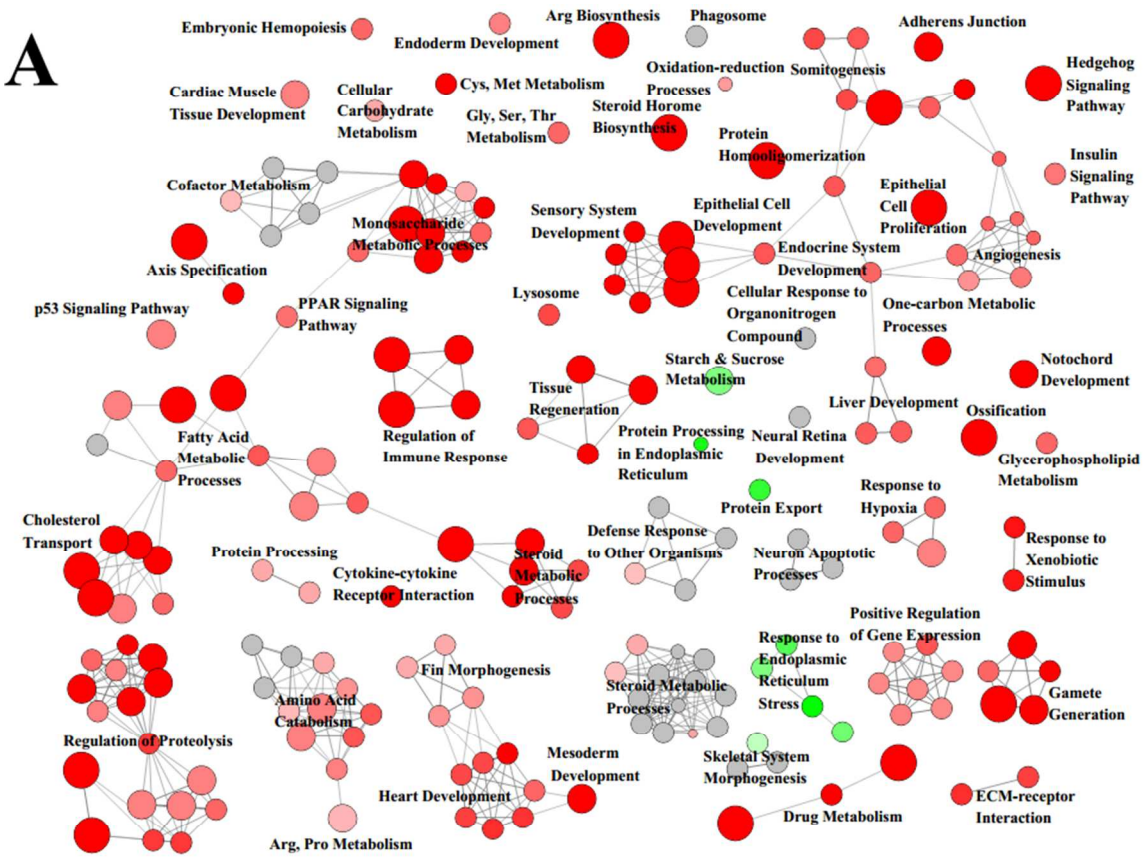
A
Embryonic Hemopoiesis
Endoderm Development
Arg Biosynthesis
Phagosome
Adherens Junction
Cardiac Muscle Tissue Development
Cellular Carbohydrate Metabolism
Cys, Met Metabolism
Gly, Ser, Thr Metabolism
Oxidation-reduction Processes
Steroid Horome Biosynthesis
Somitogenesis
Hedgehog Signaling Pathway
Protein Homooligomerization
Insulin Signaling Pathway
Cofactor Metabolism
Monosaccharide Metabolic Processes
Sensory System Development
Epithelial Cell Development
Epithelial Cell Proliferation
Axis Specification
Endocrine System Development
Angiogenesis
Lysosome
Cellular Response to Organonitrogen Compound
p53 Signaling Pathway
PPAR Signaling Pathway
One-carbon Metabolic Processes
Starch & Sucrose Metabolism
Notochord Development
Tissue Regeneration
Liver Development
Ossification
Fatty Acid Metabolic Processes
Regulation of Immune Response
Protein Processing in Endoplasmic Reticulum
Neural Retina Development
Glycerophospholipid Metabolism
Protein Export
Response to Hypoxia
Cholesterol Transport
Defense Response to Other Organisms
Protein Processing
Steroid Metabolic Processes
Neuron Apoptotic Processes
Response to Xenobiotic Stimulus
Cytokine-cytokine Receptor Interaction
Positive Regulation of Gene Expression
Response to Endoplasmic Reticulum Stress
Fin Morphogenesis
Amino Acid Catabolism
Steroid Metabolic Processes
Gamete Generation
Regulation of Proteolysis
Mesoderm Development
Skeletal System Morphogenesis
Heart Development
Drug Metabolism
ECM-receptor Interaction
Arg, Pro Metabolism

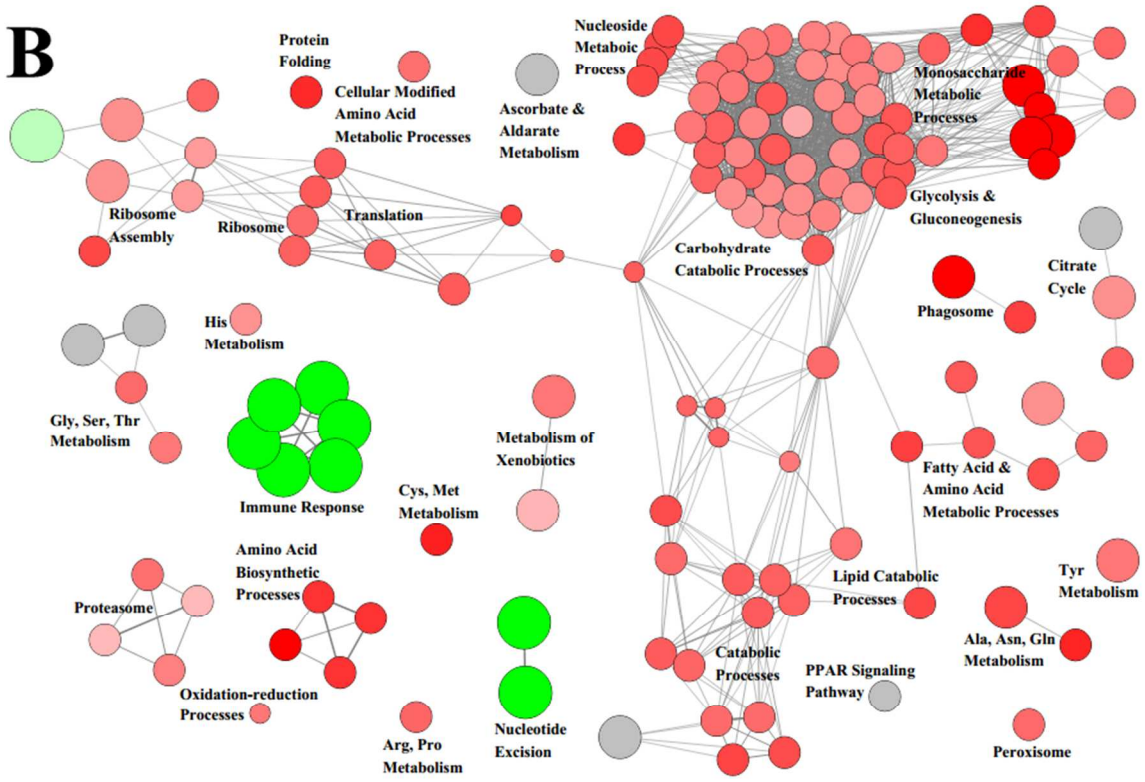
B
Protein Folding
Cellular Modified Amino Acid Metabolic Processes
Nucleoside Metaboic Process
Ascorbate & Aldarate Metabolism
Monosaccharide Metabolic Processes
Ribosome Assembly
Ribosome
Translation
Glycolysis & Gluconeogenesis
Carbohydrate Catabolic Processes
Citrate Cycle
Phagosome
His Metabolism
Gly, Ser, Thr Metabolism
Metabolism of Xenobiotics
Immune Response
Fatty Acid & Amino Acid Metabolic Processes
Cys, Met Metabolism
Amino Acid Biosynthetic Processes
Lipid Catabolic Processes
Tyr Metabolism
Proteasome
Ala, Asn, Gln Metabolism
Catabolic Processes
PPAR Signaling Pathway
Oxidation-reduction Processes
Nucleotide Excision
Arg, Pro Metabolism
Peroxisome

Figure S9 Cytoscape visualization of ClueGO clustering results of physiological processes altered by PCB 77 at the level of the transcriptome (A) and proteome (B) in liver of white sturgeon. Clusters with a greater proportion of up-regulated processes are shown in (red) while clusters with a greater proportion of down-regulated processes are shown in (green). Degree of red or green shows relative abundance of up-regulated vs down-regulated processes in each cluster. Grey clusters consist of 50% up-regulated processes and 50% down-regulated processes. Size of cluster represents the relative number of processes in the cluster. Interconnection between pathways is represented by grey interconnecting lines indicating that these categories share transcript(s) or protein(s).

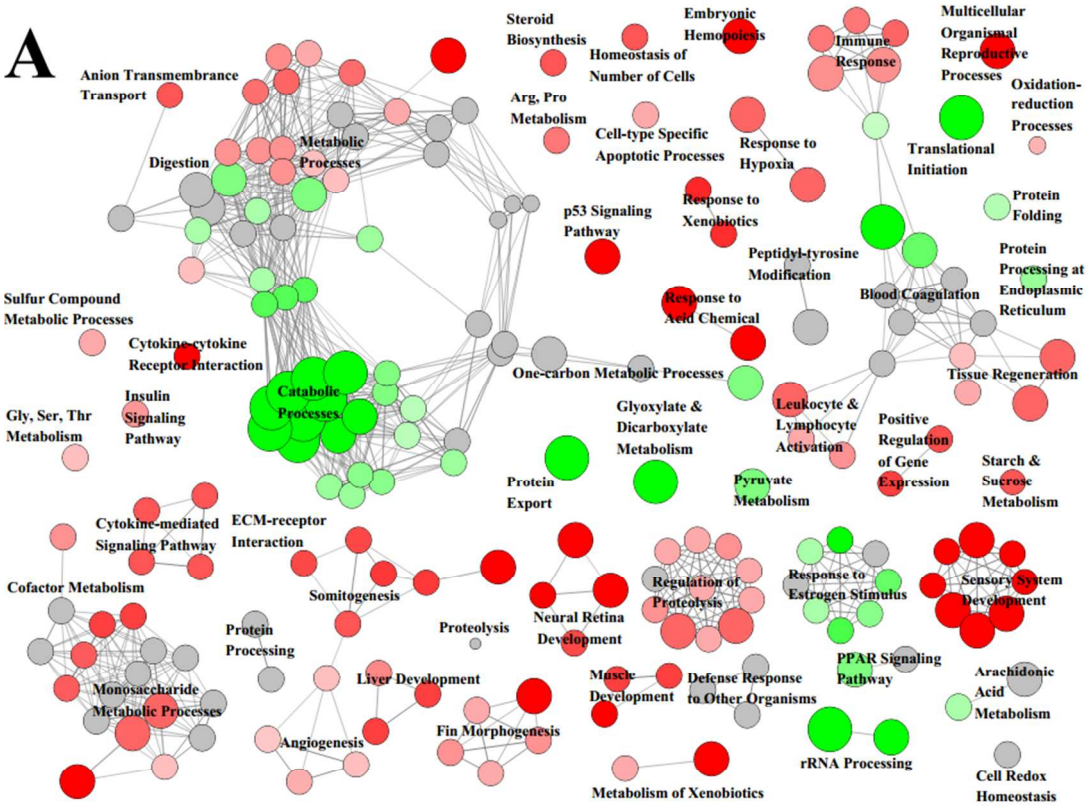
A
Anion Transmembrance Transport
Digestion
Metabolic Processes
Steroid Biosynthesis
Homeostasis of Number of Cells
Embryonic Hemopoiesis
Immune Response
Multicellular Organismal Reproductive Processes
Oxidation-reduction Processes
Arg, Pro Metabolism
Cell-type Specific Apoptotic Processes
Response to Hypoxia
Translational Initiation
p53 Signaling Pathway
Response to Xenobiotics
Protein Folding
Peptidyl-tyrosine Modification
Protein Processing at Endoplasmic Reticulum
Blood Coagulation
Sulfur Compound Metabolic Processes
Response to Acid Chemical
Cytokine-cytokine Receptor Interaction
One-carbon Metabolic Processes
Tissue Regeneration
Catabolic Processes
Insulin Signaling Pathway
Gly, Ser, Thr Metabolism
Glyoxylate & Dicarboxylate Metabolism
Leukocyte & Lymphocyte Activation
Positive Regulation of Gene Expression
Protein Export
Pyruvate Metabolism
Starch & Sucrose Metabolism
Cytokine-mediated Signaling Pathway
ECM-receptor Interaction
Cofactor Metabolism
Somitogenesis
Regulation of Proteolysis
Response to Estrogen Stimulus
Sensory System Development
Protein Processing
Proteolysis
Neural Retina Development
PPAR Signaling Pathway
Arachidonic Acid Metabolism
Monosaccharide Metabolic Processes
Liver Development
Muscle Development
Defense Response to Other Organisms
Angiogenesis
Fin Morphogenesis
rRNA Processing
Cell Redox Homeostasis
Metabolism of Xenobiotics
B
PPAR Signaling Pathway
Ribosome Assembly
Arg & Pro Metabolism
Gly, Ser, Thr Metabolism
Cellular Modified Amino Acid Biosynthetic Processes
Pentose Phosphate Pathway
Monosaccharide Metabolic Processes
Translation
Citrate Cycle
Trp Metabolism
Metabolism of Xenobiotics
Glycolysis & Gluconeogenesis
Fatty Acid & Amino Acid Degradation
Beta-Ala Metabolism
Carbohydrate Catabolic Processes
Organic Acid Biosynthetic Process
Immune Response
Lipid Catabolic Process
Nucleoside Metabolic Processes
Ascorbate & Aldarate Metabolism
Proteasome
Amino Acid Metabolism
Protein Polymerization
Amino Acid Catabolic Processes
Pyruvate Metabolism
Oxidation-reduction Processes
Peroxisome
Aerobic Respiration
His Metabolism
Lysosome

Figure S10 Cytoscape visualization of ClueGO clustering results of physiological processes altered by BaP at the level of the transcriptome (A) and proteome (B) in liver of white sturgeon. Clusters with a greater proportion of up-regulated processes are shown in (red) while clusters with a greater proportion of down-regulated processes are shown in (green). Degree of red or green shows relative abundance of up-regulated vs down-regulated processes in each cluster. Grey clusters consist of 50% up-regulated processes and 50% down-regulated processes. Size of cluster represents the relative number of processes in the cluster. Interconnection between pathways is represented by grey interconnecting lines indicating that these categories share transcript(s) or protein(s).

REFERENCES

(1) Doering J.A.; Wiseman S; Beitel S.C.; Giesy, J.P.; Hecker M. Identification and expression of aryl hydrocarbon receptors (AhR1 and AhR2) provide insight in an evolutionary context regarding sensitivity of white sturgeon (*Acipenser transmontanus*) to dioxin-like compounds. *Aquat. Toxicol.* **2014**, 150, 27-35.

(2) Conesa, A., Gotz, S., Garcia-gomez, J.M., Terol, J., Talon, M., Robles, M. Blast2GO: a universal tool for annotation, visualization and analysis in functional genomics research. Bioinformatics. **2005**, 21, 3674-3676.

(3) Robinson, M.D.; McCarthy, D.J.; Smyth, G.K. edgeR: a Bioconductor package for differential expression analysis of digital gene expression data. *Bioinformatics*. **2010**, 26(1), 139-140.

(4) Doering, J.A.; Wiseman, S.; Beitel, S.C.; Tendler, B.J.; Giesy, J.P.; Hecker, M. Tissue specificity of aryl hydrocarbon receptor (AhR) mediated responses and relative sensitivity of white sturgeon (*Acipenser transmontanus*) to an AhR agonist. *Aquat. Toxicol.* **2012**, 114-115, 125-133.

(5) Eisner, B.K.; Doering, J.A.; Beitel, S.C.; Wiseman, S.; Raine, J.C.; Hecker, M. Cross-species comparison of relative potencies and relative sensitivities of fishes to dibenzo-p-dioxins, dibenzofurans, and polychlorinated biphenyls in vitro. *Enviro. Toxicol. Chem.* **2016**, 35(1), 173-181.

(6) Rozen, S.; Skaletsky, H.J. Primer3 on the WWW for general users and for biologist programmers. In: Krawetz, S., Misener, S. (Eds.), *Bioinformatics Methods and Protocols: Methods in Molecular Biology*. **2000**, Humana Press, NJ, USA, Available from: http://fokker.wi.mit.edu/primer3/.

(7) Simon, P. Processing quantitative real-time RT-PCR data. *Bioinformatics*. **2003**, 19: 1439-1440.

(8) Bradford, M.M. A rapid and sensitive method for the quantification of microgram quantities of protein utilizing the principle of protein-dye binding. *Anal. Biochem.* **1976**, 72, 248-254.

(9) Vizcaino, J.A.; Deutsch, E.W.; Wang, R.; Csordas, A.; Reisinger, F.; Rios, D; Dianes, J.A.; Sun, Z.; Farrah, T.; Bandeira, N.; Binz, P.A.; Xenarios, I.; Eisenacher, M.; Mayer, G.; Gatto, L.; Campos, A.; Chalkley, R.J.; Kraus, H.J.; Albar, J.P.; Martinez-Bartolome, S.; Apweiler, R.; Omenn, G.S.; Martens, L.; Jones, A.R.; Hermjakob, H. ProteomeXchanger provides globally coordinated proteomics data submission and dissemination. *Nat. Biotechnol.* **2014**, 32(3), 223-226.

(10) Wuhr, M., Freeman Jr., R.M., Presler, M., Horb, M.E., Peshkin, L., Gygi, S.P., Kirschner, M.W. Deep proteomics of the Xenopus laevis egg using an mRNA-derived reference database. Curr Biol. **2014**, 24(13), 1467-1475.

(11) Cox, J.; Mann, M. MaxQuant enables high peptide identification rates, individualized p.p.b.-range mass accuracies and proteome-wide protein quantification. Nature Biotechnology. **2008**, 26: 1367-1372.

(12) Chen, H; Boutros, P.C. VennDiagram: a package for the generation of highly-customizable Venn and Euler diagrams in R. *BMC Bioinformatics*. **2011**, 12, 35.

(13) Dray, S., Dufour, A.B. The ade4 package: Implementing the duality diagram for ecologists. J. Stat. Softw. **2007**, 22, 1-20.